Check for updates

View Article Online
View Journal

Materials Advances

Accepted Manuscript

This article can be cited before page numbers have been issued, to do this please use: A. M. Sai Krishna, K. B. Busi, G. Dalapati and S. Chakrabortty, *Mater. Adv.*, 2026, DOI: 10.1039/D6MA00191B.

This is an Accepted Manuscript, which has been through the Royal Society of Chemistry peer review process and has been accepted for publication.

Accepted Manuscripts are published online shortly after acceptance, before technical editing, formatting and proof reading. Using this free service, authors can make their results available to the community, in citable form, before we publish the edited article. We will replace this Accepted Manuscript with the edited and formatted Advance Article as soon as it is available.

You can find more information about Accepted Manuscripts in the Information for Authors.

Please note that technical editing may introduce minor changes to the text and/or graphics, which may alter content. The journal's standard Terms & Conditions and the Ethical guidelines still apply. In no event shall the Royal Society of Chemistry be held responsible for any errors or omissions in this Accepted Manuscript or any consequences arising from the use of any information it contains.

ROYAL SOCIETY OF CHEMISTRY

rsc.li/materials-advances

View Article Online
DOI: 10.1039/D6MA00191B

Solar-Light-Driven Photocatalytic Water Splitting Using CuS/ZnS Type II Heterojunction: A Route to Green Hydrogen Production

Ambati Mounika Sai Krishna,[1] *Kumar Babu Busi,*[2] *Goutam Kumar Dalapati,*[3,4] *Sabyasachi Chakrabortty,*[2,5,*]

[1] Department of Physics, School of Engineering and Sciences (SEAS), SRM University AP, Amaravati 522240, Andhra Pradesh, India

[2] Department of Chemistry, School of Engineering and Sciences (SEAS), SRM University AP, Amaravati 522240, Andhra Pradesh, India

[3] Center of Nanofibers and Nanotechnology, Mechanical Engineering Department, National University of Singapore – 117576.

[4] Hydrogen Innovation Pte. Ltd., Singapore, 637141, Singapore

[5] Centre for Interdisciplinary Research, SRM University AP, Amaravati 522240, Andhra Pradesh, India

***Corresponding author:** sabyasachi.c@srmap.edu.in

Open Access Article. Published on 20 June 2026. Downloaded on 6/20/2026 11:52:44 PM.
This article is licensed under a Creative Commons Attribution-NonCommercial 3.0 Unported Licence.

Materials Advances Accepted Manuscript

View Article Online
DOI: 10.1039/D6MA00191B

Open Access Article. Published on 20 June 2026. Downloaded on 6/20/2026 11:52:44 PM.
This article is licensed under a Creative Commons Attribution-NonCommercial 3.0 Unported Licence.

Materials Advances Accepted Manuscript

View Article Online
DOI: 10.1039/D6MA00191B

Open Access Article. Published on 20 June 2026. Downloaded on 6/20/2026 11:52:44 PM.
This article is licensed under a Creative Commons Attribution-NonCommercial 3.0 Unported Licence.

Materials Advances Accepted Manuscript

Abstract:

The efficacy of photocatalysts for green hydrogen (H_2) production by solar-driven photocatalytic water splitting is still severely limited by ineffective charge separation, quick charge carrier recombination and low structural stability. In this study, a simple, low-temperature hydrothermal synthesis of CuS and ZnS (CZS) was used to rationally design a heterojunction photocatalyst, providing a simple and scalable method for improved photocatalytic performance. After 12 hours of continuous 1-sun irradiation, the CZS nanocomposite showed a remarkable cumulative H_2 production of 12,145 μmol g^{-1} which is more activity than the pristine CuS and ZnS. Additionally, the CZS heterojunction nanostructure has ~0.16% of solar to hydrogen efficiency (STH). Extensive structural and spectroscopic investigations, including as XRD, TEM, UV-Vis absorption spectroscopy and XPS revealed the CZS confirms the formation of structured system with strong interfacial interactions. The proposed composite has a unique physicochemical characteristics and synergistic interactions, supporting its increased photocatalytic activity. Improved light absorption and effective interfacial charge separation within the composite are the responsible for increased photocatalytic performance. This work highlights the efficient and scalable solutions for solar-driven H_2 production with earth-abundant sulphide materials for a viability hetero-structured system. This type of system with synergistic characteristics paves the path for a sustainable world towards decarbonization.

Keywords: Water splitting, Photocatalysis, Hydrogen evolution, CuS/ZnS composite, Type II - heterojunction.

View Article Online
DOI: 10.1039/D6MA00191B

Open Access Article. Published on 20 June 2026. Downloaded on 6/20/2026 11:52:44 PM.
This article is licensed under a Creative Commons Attribution-NonCommercial 3.0 Unported Licence.

Materials Advances Accepted Manuscript

1. Introduction

Fossil fuels that are used excessively release harmful gaseous pollutants (such as., CO, NOx, CO_2 and SO_2) into the atmosphere. By intensifying the greenhouse effect and generating global warming and environmental degradation,(1,2) these pollutants are contributing factor to anthropogenic climate change. To mitigate these adverse impacts and ensure long-term environmental sustainability, the exploration and development of clean, renewable and sustainable energy alternatives have become imperative. Green hydrogen (H_2) production through renewable energy sources (solar, wind, water, biomass, geothermal) is a promising alternative to the fossil fuels.(3) Among the numerous energy sources, production of H_2 through water is consider as more effective, because of its high abundance and the byproduct is only oxygen (O_2), which is net-zero emission of CO_2.(4) H_2 evolution by water splitting are of three types: (i) photocatalysis (PC), (ii) electrocatalysis (EC) and (iii) photo-electrocatalysis (PEC).(5),(6) Among the three water electrolysis techniques, PC water splitting has emerged as a promising route for sustainable green H_2 production due to its ability to directly utilize solar energy to drive water dissociation. By harnessing a broad solar spectrum, this process efficiently generates photoexcited charge carriers, facilitating the redox reactions required for H_2 evolution without fossil fuel combustion.(7–10) However, photocatalysts play an important role in this process by absorbing light energy, separating charges (electrons (e^-) and holes (h^+)), and generating charge carriers that can then engage in redox processes to produce H_2 or O_2.(11,12) Nanostructured materials have garnered immense interest in photocatalytic H_2 production due to their tunable morphology, quantum confinement effects, high surface-to-volume ratio, and enhanced charge carrier dynamics. Various nano-photocatalysts, including transition metal oxides, sulphides, carbides, nitrides, selenides, chalcogenides and carbon-based nanomaterials, have been extensively explored for solar-driven water splitting. However, broad bandgaps, poor visible light absorption and a rapid charge carrier recombination of

View Article Online
DOI: 10.1039/D6MA00191B

Open Access Article. Published on 20 June 2026. Downloaded on 6/20/2026 11:52:44 PM.
This article is licensed under a Creative Commons Attribution-NonCommercial 3.0 Unported Licence.

Materials Advances Accepted Manuscript

several photocatalysts typically restrict practical efficiency, which causes suboptimal H_2 evolution rates. To overcome these limitations, strategies such as surface functionalization, heterojunction engineering, bandgap engineering and co-catalyst integration have been explored to enhance the light harvesting and charge separation for improved photocatalytic performance. A semiconductor heterojunction has demonstrated as a successful and effective in enhancing the photocatalytic performance.(13)(14)(15) When two semiconductors with distinct electrical structures brought into close proximity to one another, heterojunction is created that permits interfacial charge transfer and the spatial separation of photogenerated electrons and holes. In addition, this separation not only offers a greater number of charge carriers for redox process but also prevents the recombination. A various mechanism, such as Type-II heterojunction or Z-scheme systems, may function depending on band alignment, each offering a distinct benefit in form of redox potential and charge separation. The fabrication of advanced heterostructure photocatalyst, such as low-dimensional materials and sulphide-based composites has received a potential attention in recent years. However, despite these developments, there are still some major challenges. Metal sulphide photocatalyst in particular are vulnerable to photo-corrosion, which can lead to activity loss and structural degradation. Furthermore, many photocatalytic systems depend on sacrificial agents to prevent the charge recombination, which restricts their sustainability and practical applicability. Therefore, developing a photocatalyst that combine effective charge separation, structural stability and economical synthesis still remains an ongoing challenge. Among various semiconductor materials, transition metal sulphides are considered to be a favourable candidate for photocatalytic H_2 evolution due to its ideal conduction band positions for water reduction.(16) From the last two decades, different research groups worked on diverse metal sulphides, such as., MoS_2, CdS, WS_2, In_2S_3, $ZnIn_2S_4$, NiS_2, however the overall efficiency was not up to the standard due to their limitations. Despite having a strong optical absorption, but sometimes low

View Article Online
DOI: 10.1039/D6MA00191B

Open Access Article. Published on 20 June 2026. Downloaded on 6/20/2026 11:52:44 PM.
This article is licensed under a Creative Commons Attribution-NonCommercial 3.0 Unported Licence.

Materials Advances Accepted Manuscript

active site density and unstable working circumstances of metal sulphides make it difficult to use them practically in photocatalytic processes. These materials long-term performance and efficiency are significantly impacted by their extreme susceptibility to photoinduced corrosion, oxidation and structural degradation.(17) Furthermore, many reported systems rely on the sacrificial agents to prevent the recombination, which restricts their sustainability and scalability for practical uses. Zinc sulphide (ZnS) is a potential semiconductor material due to its wide range of applications in optoelectronics, photocatalysis, and sensing. However, its broad bandgap of 3.72 eV restricts its absorption to the ultraviolet (UV) region, limiting its usefulness in visible-light-based applications.(18) A number of research groups have worked on this catalyst, refining the physicochemical properties and tweaking or generating defect sites (Zn and S vacancies) to increase the H_2 evolution rate. For example, Hao et al., optimized the Zn vacancies in ZnS (irregular morphology) and it has 337.71 μmol h^{-1} g^{-1} maximum H_2 production rate under visible light.(19) Wang et al., produced S vacancies in ZnS structure (spherical morphology) to extend the absorption of light in visible range to enhance the H_2 rate, but it gives only 232 μmol h^{-1} g^{-1}.(20) Xu et al., developed a single phase of ZnS (hollow microspheres) with high porosity and surface area and reported 1.66 μmol h^{-1} g^{-1} H_2 production rate under UV.(21) Based on the literature, bare ZnS is having low H_2 evolution rate, because of its band gap, can responds only to the UV light which is its major limitation in practical application. It also suffers from the rapid recombination of photoexcited electrons and holes, photo-corrosion and poor charge transport. Therefore, to enhance photocatalytic H_2 production, the rational design of hybrid photocatalysts through nanoengineering strategies such as heterojunction formation, composite fabrication, alloying, and elemental doping can significantly improve catalytic efficiency.

To address these limitations, coupling bare ZnS with a narrow bandgap semiconductor is an effective strategy. Formation of heterojunctions between two nanomaterials can

View Article Online
DOI: 10.1039/D6MA00191B

efficiently separate charges by directing photoexcited electrons (e^-) towards one component and holes (h^+) towards another, reducing charge recombination and improving redox processes. Such developments allow for increased light absorption, enhanced band structure, and improved surface reaction kinetics, making them ideal for solar-driven water splitting and sustainable hydrogen generation.(22), (23) However, copper sulphide (CuS) was chosen as an alternative for altering the light absorption properties of ZnS nanostructures as composites. CuS is a narrow band gap semiconductor with 1.5 eV to 2.0 eV(24,25) band gap which makes a suitable candidate for visible to near infrared (NIR) light photocatalysis application. Interestingly, according to the earlier reports, CuS has exceptional photo-physical properties, where more photons captured at the NIR range due to localized surface plasmon resonance.(26) Integrating the CuS with ZnS will helps in formation of CuS/ZnS (CZS) hetero-structured composite. This CZS heterostructure increases the efficient separation of photo-triggered charge carriers at the interface. The findings contribute to a better understanding of charge separation efficiency and a significant alteration in the rate of recombination of a photo-triggered charge carriers, which are the major factors in photocatalysis.(27) Also, this multi-metal chalcogenide combination will possess the low-toxicity, high stability, more photo-conductivity and strong photo response towards the visible light.(28) The formation of interfacial contact has a more advantage for composite photocatalyst in promoting the separation of photogenerated electron-hole pairs, which enhances the photocatalysis efficiency. Thus, a hetero-structured CZS composite photocatalyst would facilitate an excellent photocatalytic H_2 production activity by employing a sustainable route of photocatalytic water splitting.

In general, heterojunction formation between two distinct materials as a photocatalyst will provide attractive features including wide range of light absorption, sufficient active sites, reduced charge recombination, and better stability. Such photocatalysts would improve the

Open Access Article. Published on 20 June 2026. Downloaded on 6/20/2026 11:52:44 PM.
This article is licensed under a Creative Commons Attribution-NonCommercial 3.0 Unported Licence.

Materials Advances Accepted Manuscript

View Article Online
DOI: 10.1039/D6MA00191B

photocatalytic activity and enhances the green energy generation. In that perspective, a composite was prepared using a simple single pot hydrothermal technique at low temperature with CuS and ZnS metal sulphides (CZS hetero-structured composite photocatalyst) to improve the photocatalytic H_2 evolution. The optical and electronic properties of the CZS photocatalyst was characterized by various techniques such as XRD, SEM, TEM, UV-Vis absorbance, and XPS. Based on the different characterization, it was confirmed that the as-synthesized photocatalyst is having a synergistic and unique physicochemical property. This synergistic effect will have high light harvesting, enhanced charge mobility and reduced recombination at interface. The unique properties of CZS composite shows an efficient charge separation at the interface and expected to enhance the photocatalytic activity. Also, the photocatalytic experiments were conducted in photochemical reactor under the continuous illumination of 1 sun light source which results an increased photocatalytic H_2 production compared to the control ZnS and CuS photocatalysts. The proposed system offers an advantage including simple synthesis, utilization of relatively abundant materials and improved light-harvesting capability. The purpose of this present work is to provide insight into the significance of interfacial charge transfer in hetero-structured photocatalyst and facilitate in the formation of an effective solar-driven H_2 production systems. Also, this type of a metal composite photocatalyst with unique properties and synergistic effects between the components opens a new route for a sustainable production of H_2 and pollutant free nature.

2. Experimental Section

2.1 Synthetic procedure:

A robust CZS nanocomposite photocatalyst was synthesized using a simple hydrothermal technique for efficient water splitting to generate chemical commodities as shown in **scheme 1**. The synthesis steps used to generate CZS composite are as follows: first,

Open Access Article. Published on 20 June 2026. Downloaded on 6/20/2026 11:52:44 PM.
This article is licensed under a Creative Commons Attribution-NonCommercial 3.0 Unported Licence.

Materials Advances Accepted Manuscript

View Article Online
DOI: 10.1039/D6MA00191B

0.5 M of Na_2S was dissolved in a 1:1 mixture of 20 mL of E.G and 20 mL of D.I water with intense sonication until it totally dissolves. In the second step, 0.5 M of $ZnCl_2$ and $CuCl_2$ was added to the above mixture one by one and stirred the solution until it turns into the transparent. Later, the resultant mixture was transferred into the 100 mL of teflon-lined stainless-steel autoclave and the autoclave was treated at 180°C for 60 minutes. Once the hydrothermal reactor cooldown, the resultant mixture was washed for several times with D.I water and ethanol. Finally, the resultant mixture was dried for overnight in hot air oven at 60°C, to get the final CZS nanocomposite photocatalyst. Similarly, CuS photocatalyst was synthesized by following the same procedure but without the addition of Zn precursor and ZnS photocatalyst without Cu precursor.

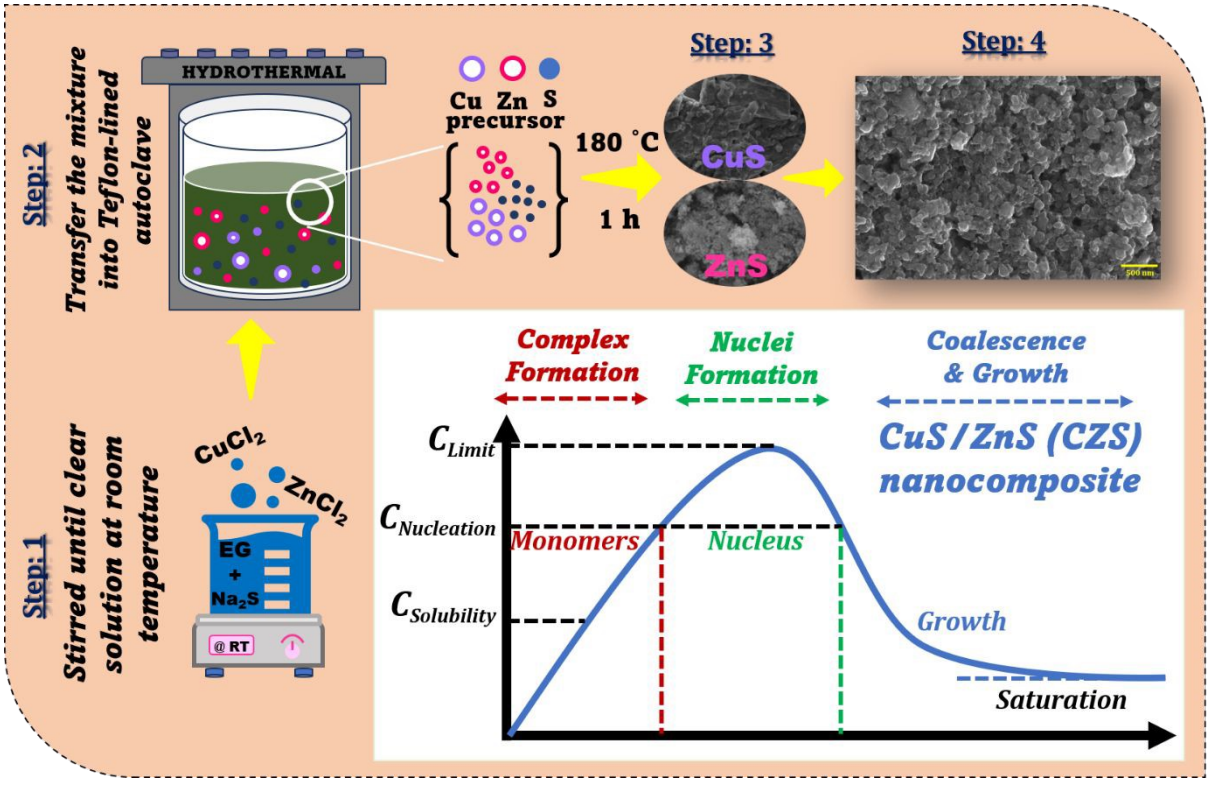

Scheme 1: Above figure shows the representation of various steps included in CuS/ZnS (CZS) nanocomposite material prepared using a simple and straight forward in-situ synthesis process via hydrothermal technique. The nucleation and particle growth procedure also included as an inlet figure.

2.2 Photocatalysis measurement (PC):

Open Access Article. Published on 20 June 2026. Downloaded on 6/20/2026 11:52:44 PM.
This article is licensed under a Creative Commons Attribution-NonCommercial 3.0 Unported Licence.

Materials Advances Accepted Manuscript

View Article Online
DOI: 10.1039/D6MA00191B

Open Access Article. Published on 20 June 2026. Downloaded on 6/20/2026 11:52:44 PM.
This article is licensed under a Creative Commons Attribution-NonCommercial 3.0 Unported Licence.

In this study, the efficient production of green H_2 was measured utilizing CZS nanocomposite as a photocatalyst via photocatalytic water splitting process. A photochemical reactor was employed beneath the light source supplied by the solar simulator, and the full reaction setup is depicted in **Figure S5**. To flush out the other gases, the photochemical reactor was purged with nitrogen about 20 mins and illuminated by one SUN of AM 1.5 G. However, 20 mg of CZS photocatalyst was mixed in 2 mL of aqueous solution (typical concentration – 10 mg/mL), containing 0.1M of Na_2SO_4 as a sacrificial electron donor (SED) agent before being transferred into the photochemical reactor. Throughout the process, the reaction solution was continuously stirred with a magnetic stirrer to provide better light exposure of light to the photocatalyst with the assistance of magnetic stirrer and maintained constant at room temperature. Finally, the evolved gas measurements were taken in an airtight syringe and separated using offline gas chromatography (GC). The thermal conductivity detector (TCD) has been employed to detect the evolved H_2 gas from the photocatalyst, and the measurement data were taken at a regular time interval of every 3 hours until the measurement was completed (12 hours).

3. Results and Discussion

3.1 Structural analysis:

The CZS composite photocatalyst's crystalline nature, crystal structure and phase composition characteristics were investigated with x-ray diffraction (XRD) technique in θ to 2θ geometry. **Figure 1** shows the diffraction patterns of bare ZnS, CuS and CZS composite photocatalysts. The major diffraction peak of bare ZnS photocatalyst was located at 28.8°, which corresponds to (0010) lattice plane, and CuS at 48.2°, which corresponds to (110) plane. Whereas, CZS photocatalyst has a large diffraction peak at 46.5°, which corresponds to the (1013) lattice plane. The lattice planes of bare ZnS photocatalyst were matched with the JCPDS

Materials Advances Accepted Manuscript

View Article Online
DOI: 10.1039/D6MA00191B

card.no: 01-072-0162 (wurtzite – hexagonal structure) and CuS with 01-079-2321 (covellite – hexagonal structure). Meanwhile, CZS photocatalyst was matched with both the cards, indicting the formation of composite. Furthermore, peak sharpness and intensity was significantly enhanced in the case of CZS composite suggesting the formation of high crystalline nature for better catalytic performance, when compared to bare ZnS and CuS. For any catalyst, crystallinity plays a critical role in catalytic performance because severe defects in the arrangement of crystal lattice can promote electron-hole recombination, which decreases catalytic activity.(27) In addition, the diffraction peaks of bare photocatalysts CuS and ZnS showed high index facet (HIF) planes due to large density of low-coordinated surface atoms such edges, kinks, and steps possess increased surface energy, which is consistent with literature. Interestingly, after the formation of CZS composite heterojunction, most of the diffraction peaks were observed as HIF planes, which attributes to the increased surface energy and promotes more active sites for better catalytic performance. As a result, such robust catalysts are expected to allow them to serve as a novel class of materials for different catalysis, sensing, optoelectronic and energy harvesting applications.(29)

Open Access Article. Published on 20 June 2026. Downloaded on 6/20/2026 11:52:44 PM.
This article is licensed under a Creative Commons Attribution-NonCommercial 3.0 Unported Licence.

Materials Advances Accepted Manuscript

View Article Online
DOI: 10.1039/D6MA00191B

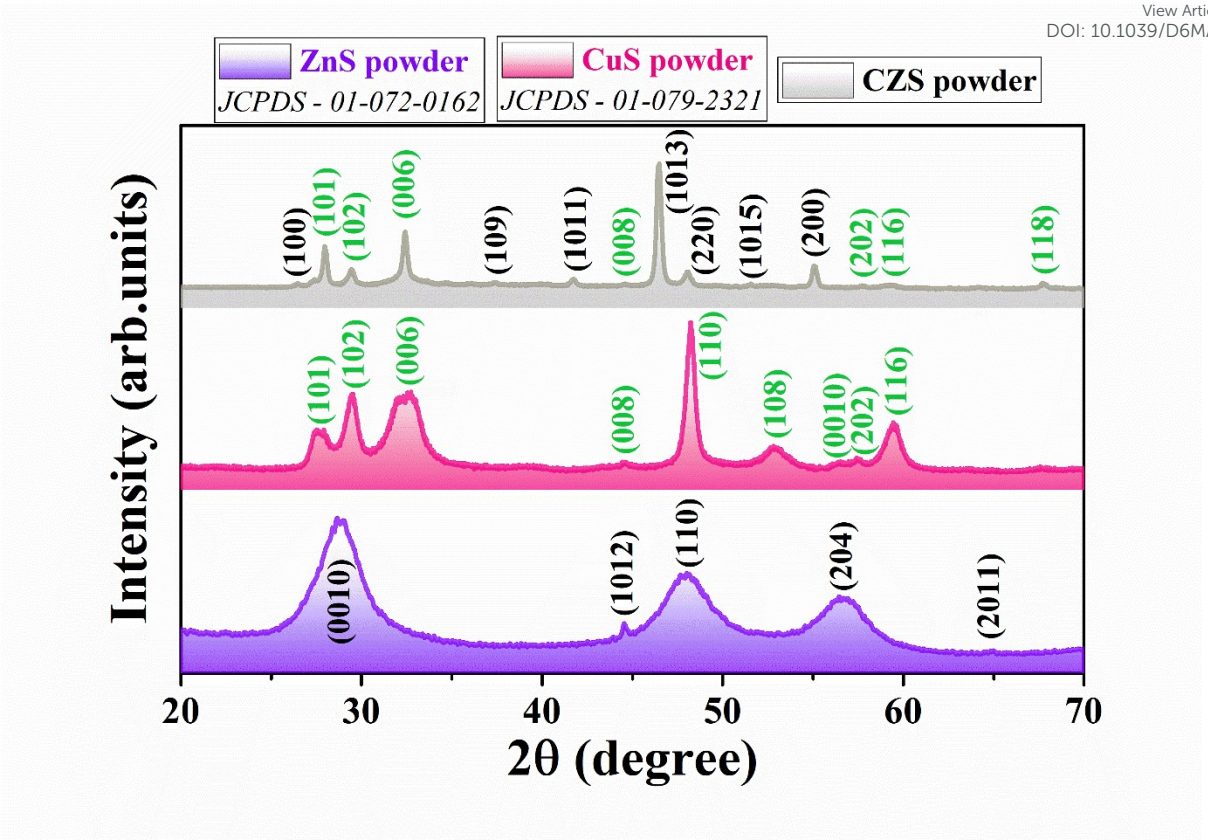

Figure 1: **Crystal lattice and structural investigation**. XRD patterns of bare ZnS (wurtzite – hexagonal structure) matched with JCPDS: 01-072-0162 and CuS with 01-079-2321 (covellite – hexagonal structure), CZS composite photocatalyst has both the phases.

In general, photocatalysts must be examined at multiple dimensions in order to comprehend their microstructural information at both electronic and atomic levels, which provide better understanding of their inherent features and improves catalytic performance. The XRD technique essentially evaluates the crystal structure or crystalline materials in terms of different Bragg peaks, lattice planes, and crystal phases. Also, this technique may efficiently calculate the crucial crystal lattice characteristics including crystallite size (D), dislocation density (d), micro-strain (ε) from full-width at half-maximum (FWHM) diffraction peaks and the respective measurements CZS composite depicted in **Figure 2**.

Open Access Article. Published on 20 June 2026. Downloaded on 6/20/2026 11:52:44 PM.
This article is licensed under a Creative Commons Attribution-NonCommercial 3.0 Unported Licence.

Materials Advances Accepted Manuscript

View Article Online
DOI: 10.1039/D6MA00191B

Open Access Article. Published on 20 June 2026. Downloaded on 6/20/2026 11:52:44 PM.
This article is licensed under a Creative Commons Attribution-NonCommercial 3.0 Unported Licence.

Materials Advances Accepted Manuscript

As shown in **Figure 2(a)**, the CZS composite photocatalyst had a higher crystallite size (D) than bare ZnS and CuS photocatalysts. The composite has a D-value of 23.58 nm, compared to 3.03 nm for ZnS and 9.64 nm for CuS. A significant increase in D-values could be attributed to the formation of heterojunction between CuS and ZnS.(30,31) Such kind of an enhancement in the crystallite size promotes strong heterojunction formation by employing better interfacial contact, decreased charge recombination and providing sufficient surface area for active photocatalytic performance. The computed D-values for all three photocatalysts are listed in **Table S1, Table S2 and Table S3**. The catalyst crystalline size (D) was determined using the Debye-Scherrer formula (1). On the other hand, lattice spacing, also known as inter-atomic spacing or d-spacing, refers to the distance between parallel planes of two successive atoms or planes that result in diffraction peaks. **Figure 2(b)** presents the dislocation density of three different photocatalysts: CuS (2.16 Å), ZnS (2.21 Å), and CZS (2.18 Å). Notably, the d-spacing value of the CZS composite remains moderate, without significant increase or decrease compared to the bare catalysts. This stability suggests improved charge separation and reduced recombination rates, enhancing its photocatalytic performance. The d-spacing values were determined using the following equation (2).

The production of tiny crystallites less than 1 μm leads to the increase of lattice scattering centers, resulting in lattice defects such as dislocations. The density of dislocations (δ) can be measured as the distance between dislocation lines per unit volume of the crystal. The equation for estimating dislocation density (δ) and micro strain (ε) is as follows the equation (3). As previously stated, the crystalline size (D) of CZS composite was increased due to the formation of heterojunctions. The D-values indicate a decrease in the broadening of diffracted peaks in composite cases. **Figures 2(c)** and **2(d)** show the computed dislocation density (δ) and micro strain (ε). As crystallite size increases, the amount of point defects and dislocations along the grain boundaries decreases, resulting in lower micro strain for CZS

View Article Online
DOI: 10.1039/D6MA00191B

composite. Micro strain and dislocation density are signs of a dislocation network, with lower values indicating high-quality catalyst manufacture. Overall, the XRD investigation confirms that the annealing process reduces micro-strain and dislocation density, resulting to larger crystallites with enhanced crystallinity, fewer defects, and improved structural stability of the CZS composite heterojunction formation. This, in turn, facilitates more efficient charge transport for photocatalysis.

$$D = \frac{K\lambda}{\beta \cos\theta} \quad (1)$$

***** *D = crystallites size (nm), K = 0.9 (Scherrer constant), λ = wavelength of XRD radiation (0.154 nm), β = FWHM of peak of respective crystal lattice plane, θ = angle of the intensity peak.*

$$n\lambda = 2d \sin\theta \text{ or } d = \frac{n\lambda}{2 \sin\theta} \quad (2)$$

***** *λ = 1.5406 A◦ (incident X-ray source wavelength). d = interplanar spacing or d-spacing (in Å). n = 1 (order of diffraction). θ = Peak location (radians).*

$$\delta = \frac{1}{D^2} \text{ and } \varepsilon = \frac{\beta}{4 \cos\theta} \quad (3)$$

Open Access Article. Published on 20 June 2026. Downloaded on 6/20/2026 11:52:44 PM.
This article is licensed under a Creative Commons Attribution-NonCommercial 3.0 Unported Licence.

Materials Advances Accepted Manuscript

View Article Online
DOI: 10.1039/D6MA00191B

Open Access Article. Published on 20 June 2026. Downloaded on 6/20/2026 11:52:44 PM.
This article is licensed under a Creative Commons Attribution-NonCommercial 3.0 Unported Licence.

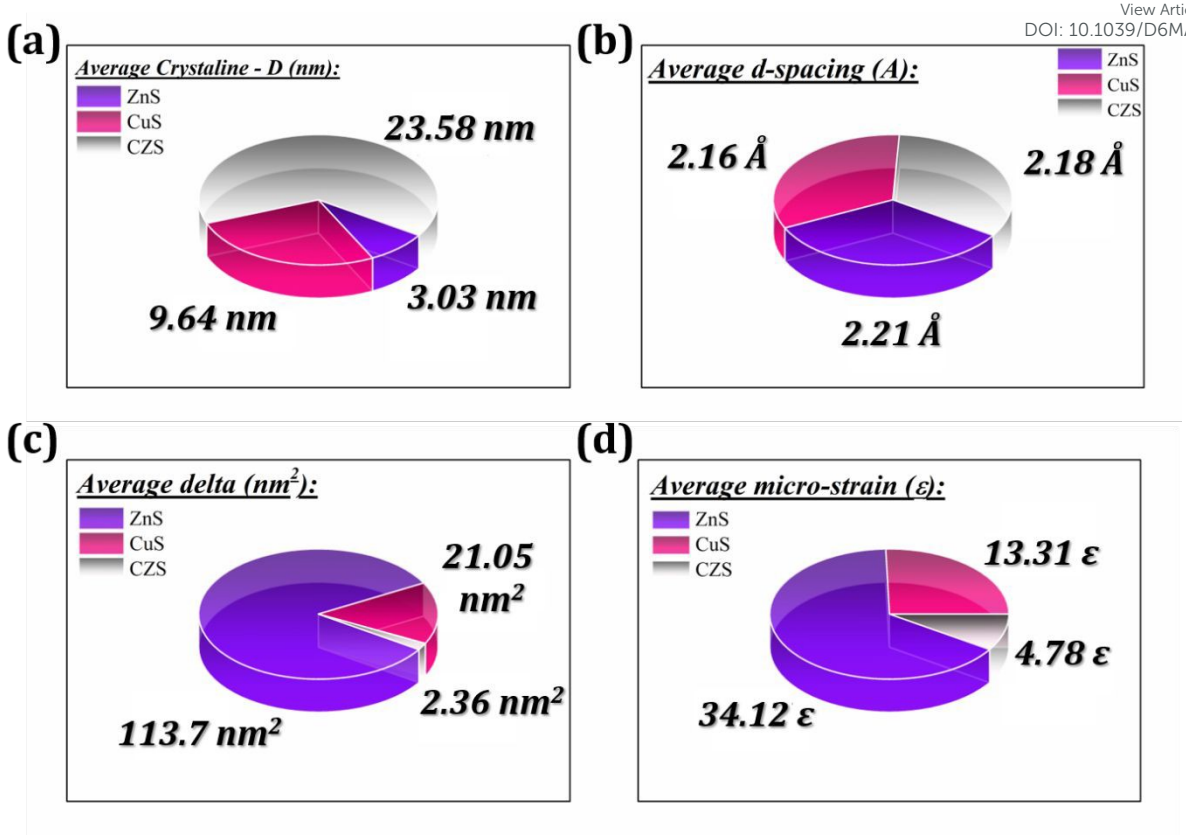

Figure 2: Structural characteristics of hydrothermally synthesized photocatalysts which includes ZnS, CuS and CZS composite. (a) average crystalline size (nm); (b) average d-spacing (Å); (c) average dislocation density (nm^2); (d) average micro-strain.

3.2 Size and morphological analysis

The morphology, microstructure and atomic arrangement properties of all three different catalysts were examined using high-resolution transmission electron microscopy (HRTEM) and scanning electron microscopy (SEM) techniques. **Figure 3** showed the plane-view HRTEM analysis with crystalline fringes of approximately 2 nm in diameter and the EDAX spectrum was showed in **Figure S1**, whereas **Figure S2** showed the SEM. **Figure 3(a)** represents the low-resolution image of ZnS nanoparticles with spherical shape and an average particle size of around 5-10 nm. **Figure 3(b)** shows the interplanar distance at 0.146 nm, 0.161 nm, and 0.204 nm corresponds to (2010), (204) and (1012) planes that belongs to the wurtzite

Materials Advances Accepted Manuscript

View Article Online
DOI: 10.1039/D6MA00191B

phase of ZnS. **Figure 3(d)** displays a low-resolution image of CuS polydisperse rod-shaped particles ranging in size from nano to microns. According to **Figure 3(e)**, the (1012), (205), and (104) planes of covellite CuS have d-spacing values of 0.125 nm, 0.146 nm, and 0.255 nm, respectively. On the other hand, **Figure 3(g)** represents a low-resolution image of CZS composite with multiple morphologies of nanospherical ZnS smaller particles and CuS plate-like particles, which evidently confirmed the formation of heterojunction between ZnS and CuS. As shown in **Figure 3(h)**, the interplanar distance of CZS composite detected at 0.135 nm corresponds to the (1,0,11) plane, which represents CuS; 0.146 nm d-spacing belongs to both the phases of ZnS (2010) and CuS (205); and 0.251 nm represents ZnS (108). The results indicated a substantial interaction between the ZnS and CuS in the composite phase. Furthermore, the selected area electron diffraction (SAED) pattern was also analyzed in order to know the crystalline nature of the photocatalysts. As showed in **Figure 3(c&f),** the SAED pattern indicates the crystalline nature of wurtzite phase of ZnS and covellite phase of CuS particles. Whereas CZS composite reveals the formation of both the phases of ZnS and CuS in multi-crystal phase (**Figure 3(i)**). All the obtained results are consistent with XRD analysis, which confirmed the high crystalline nature of composite heterojunction.

Open Access Article. Published on 20 June 2026. Downloaded on 6/20/2026 11:52:44 PM.
This article is licensed under a Creative Commons Attribution-NonCommercial 3.0 Unported Licence.

Materials Advances Accepted Manuscript

View Article Online
DOI: 10.1039/D6MA00191B

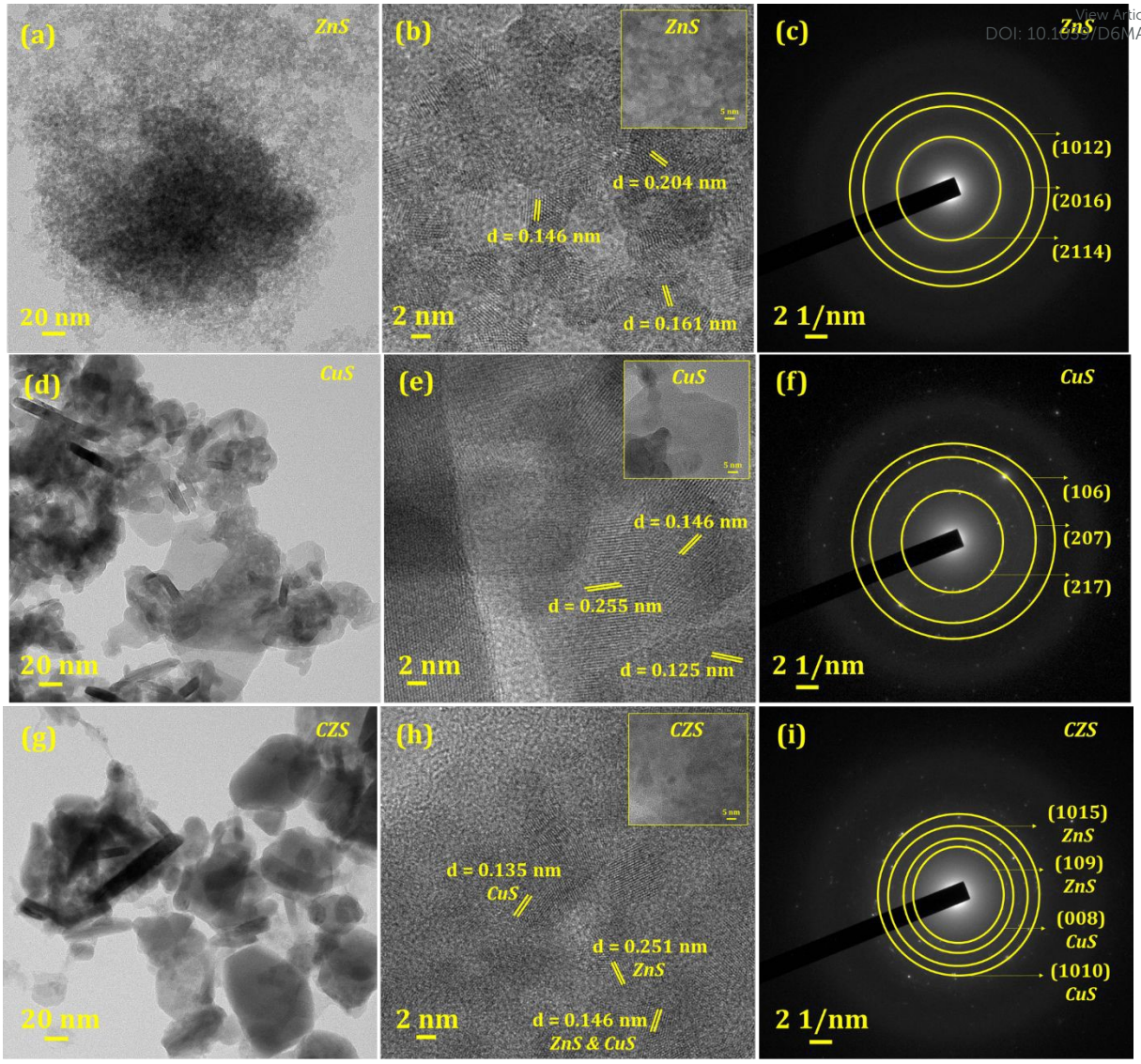

Figure 3: Morphological studies by HRTEM. (a, d, g) low resolution images of ZnS, CuS and CZS samples with 20 nm scale bar. (b, f, h) high resolution images of three catalysts ZnS, CuS and CZS with 2 nm scale bar, and the inlets with 5 nm scale bar. The d-spacing measurements of three catalysts validated the specific crystal lattice planes of ZnS, CuS and CZS. (c, f, i) SAED patterns revealed the crystalline nature of three catalysts, however CZS composite showed increased crystallinity compared to ZnS and CuS, which is consistent with XRD studies.

3.3 Optical analysis

Open Access Article. Published on 20 June 2026. Downloaded on 6/20/2026 11:52:44 PM.
This article is licensed under a Creative Commons Attribution-NonCommercial 3.0 Unported Licence.

Materials Advances Accepted Manuscript

View Article Online
DOI: 10.1039/D6MA00191B

Open Access Article. Published on 20 June 2026. Downloaded on 6/20/2026 11:52:44 PM.
This article is licensed under a Creative Commons Attribution-NonCommercial 3.0 Unported Licence.

Photocatalysts perform superior catalytic activity when they absorb the entire sunlight spectrum (Ultraviolet (UV), Visible and Infrared). **Figure 4** shows the light absorption property of three different catalysts was examined by using UV measurement technique and the respective energy gap was calculated from a diffuse reflectance measurement**.** As shown in **Figure 4(a)**, the absorption spectra of ZnS showed a UV light absorption band edge at 311 nm, while CuS showed the visible light absorption band edge at 706 nm. In contrast, CZS composite spectra revealed an increasing optical absorption band edge at 791 nm towards the near infrared (NIR) region. Compared to the bare semiconductors, the absorption edge of the CZS nanocomposite showed a red shift (around 85 nm), which is extending into NIR region. The absorption edge of CZS composite showed a red shift of around 85 nm, extending into the NIR region, as compared to the bare ZnS and CuS photocatalyst. This red shift reflects a significant electronic interaction between the two components, which may enable charge transfer across the interface (perhaps leading to formation of heterojunction) and exhibits the improved light harvesting capability. Furthermore, the improved optical absorption is expected to contribute to enhanced photocatalytic performance. The energy gap measurements of all the three photocatalysts were calculated using Tauc plots, as shown in **Figure 4(b)**. According to the energy gap measurement, CZS composite has less energy gap of ~1.4 eV, compared to CuS (~1.6 eV) and ZnS (~3.3 eV). Therefore, a catalyst with low energy gap provides a wide range of optical absorption from the solar light and vice versa at higher energy gap. Thus, a simple and straight forward in-situ synthesis of CuS-ZnS composite increased optical absorption characteristics and altered the electronic structure, allowing it to serve as a facile catalyst for photo related applications such as green energy generation and light harvesting. The band gap energy is usually determined from diffuse reflectance spectra and followed by equation (4).

$$(\alpha h\vartheta)^2 = A\,(h\vartheta - Eg) \qquad (4)$$

Materials Advances Accepted Manuscript

View Article Online
DOI: 10.1039/D5MA00191B

*α – absorbance, h – Planck constant, ϑ – photon's frequency, A – constant, Eg – band gap energy.

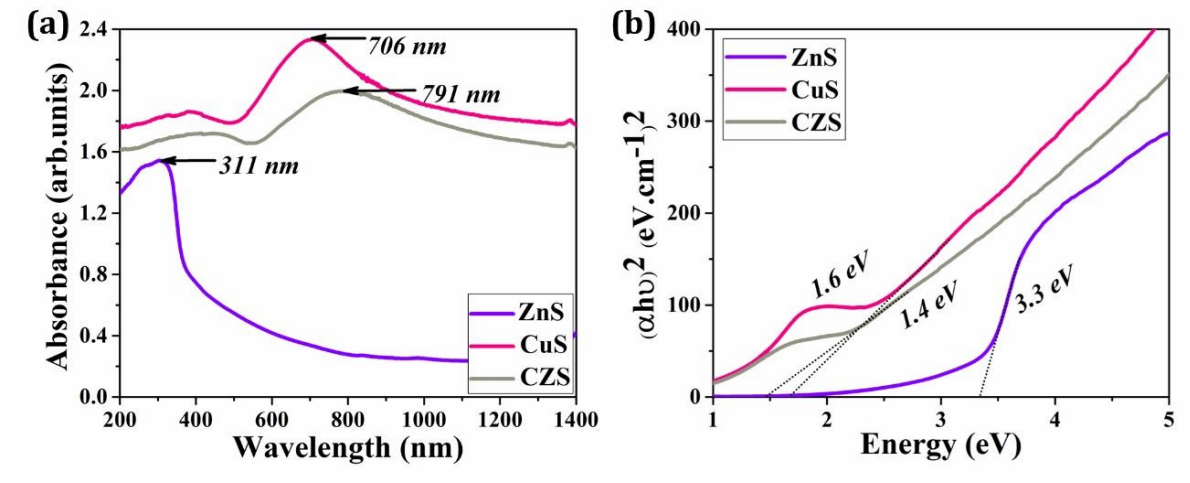

Figure 4: **Optical absorbance and bandgap measurement**. (a) Absorption spectra reveal that an increased light absorption of CZS composite photocatalyst compared to their controls ZnS and CuS. (b) Energy gap calculations of three different catalysts confirmed that CZS composite has lower energy gap allowing a wide range of light absorption.

3.4 Surface chemical composition analysis

To analyse the elemental composition and surface oxidation states of the as-synthesized CZS powder composite, x-ray photoelectron spectroscopy (XPS) technique was carried out, as illustrated in **Figure 5** and the bare ZnS, CuS full survey scan spectrum was illustrated in **Figure S3**. In this characterization technique, an incident photon energy [1486.6 eV (Al Kα)] is estimated from inelastic mean free path versus (*vs*) original electron energy (eV).(32) **Figure 5(a)** depicts the full survey spectra of CZS composite indicates the existence of various elements such as Cu 2p, Zn 2p, C 1s and S 2p. High-resolution spectral scans were precisely captured using a step interval (0.1 eV) and a pass energy (20 eV). The binding energy (BE) of Cu was mentioned in **Figure 5(b)**, peak at 932 eV and 952 eV belongs to Cu $2p_{3/2}$ and Cu $2p_{1/2}$,

Open Access Article. Published on 20 June 2026. Downloaded on 6/20/2026 11:52:44 PM.
This article is licensed under a Creative Commons Attribution-NonCommercial 3.0 Unported Licence.

Materials Advances Accepted Manuscript

View Article Online
DOI: 10.1039/D6MA00191B

respectively, which are consistent with Cu^{2+} species in CuS.(33–36) In contrast, Zn 2p signal (**Figure S4**) appears weak and less prominent in XPS spectra. This can be attributed to the surface-sensitive nature of XPS, which typically probes only the top of few nanometres of the material. The CuS species may be preferentially abundant near the surface of the composite, partially hiding the underlying ZnS phase, according to the relatively low Zn signal.(37) In general, XPS is a surface-sensitive technique (typically probing ~5 to 10 nm) and therefore primarily reflects the outermost surface composition. In contrast, EDS is bulk-sensitive technique, detaching elemental composition from deeper regions of the material. The clear Zn signal is observed in **Figure S1,** which confirms the presence of ZnS within the composite. Thus, based on the combined data of XPS and EDS, CZS composite consists of a close interfacial contact between the CuS and ZnS with a partial surface coverage. The high resolution S 2p spectrum (**Figure 5(c))** shows the divalent oxidation state at 161.5 eV (ZnS) and 162.8 eV (CuS), ascribed to S $2p_{3/2}$ in both the crystal phases, respectively.(24,34,38) As shown in **Figure 5(d)**, peak at 284 eV associated with C - C (epoxyl) and 288 eV with C=O (carbonyl) in C1s spectra is attributed to carbon peaks.(39) Interestingly, in the absence of a carbon source, the CZS composite exhibits the highest atomic fraction of C1s following hydrothermal treatment. Polymer-mediated solvents, such as EG, contain carbon-rich backbones or functional groups that may leave the catalyst with carbon residues after synthesis. As a result, during composite production, the EG solvent itself becomes a rich carbon source. This kind of composite with residual carbon may enhance the properties of photocatalyst in terms of more visible light absorption and improving the electron transfer efficiency.(40–42) As a result, the successful formation of CuS-ZnS (CZS) nanocomposite with a interfacial heterojunction features is confirmed by the observations of XPS analysis and EDS results. Therefore, this kind of a nanocomposite is advantageous for practical photocatalytic applications.

Open Access Article. Published on 20 June 2026. Downloaded on 6/20/2026 11:52:44 PM.
This article is licensed under a Creative Commons Attribution-NonCommercial 3.0 Unported Licence.

Materials Advances Accepted Manuscript

View Article Online
DOI: 10.1039/D6MA00191B

Open Access Article. Published on 20 June 2026. Downloaded on 6/20/2026 11:52:44 PM.
This article is licensed under a Creative Commons Attribution-NonCommercial 3.0 Unported Licence.

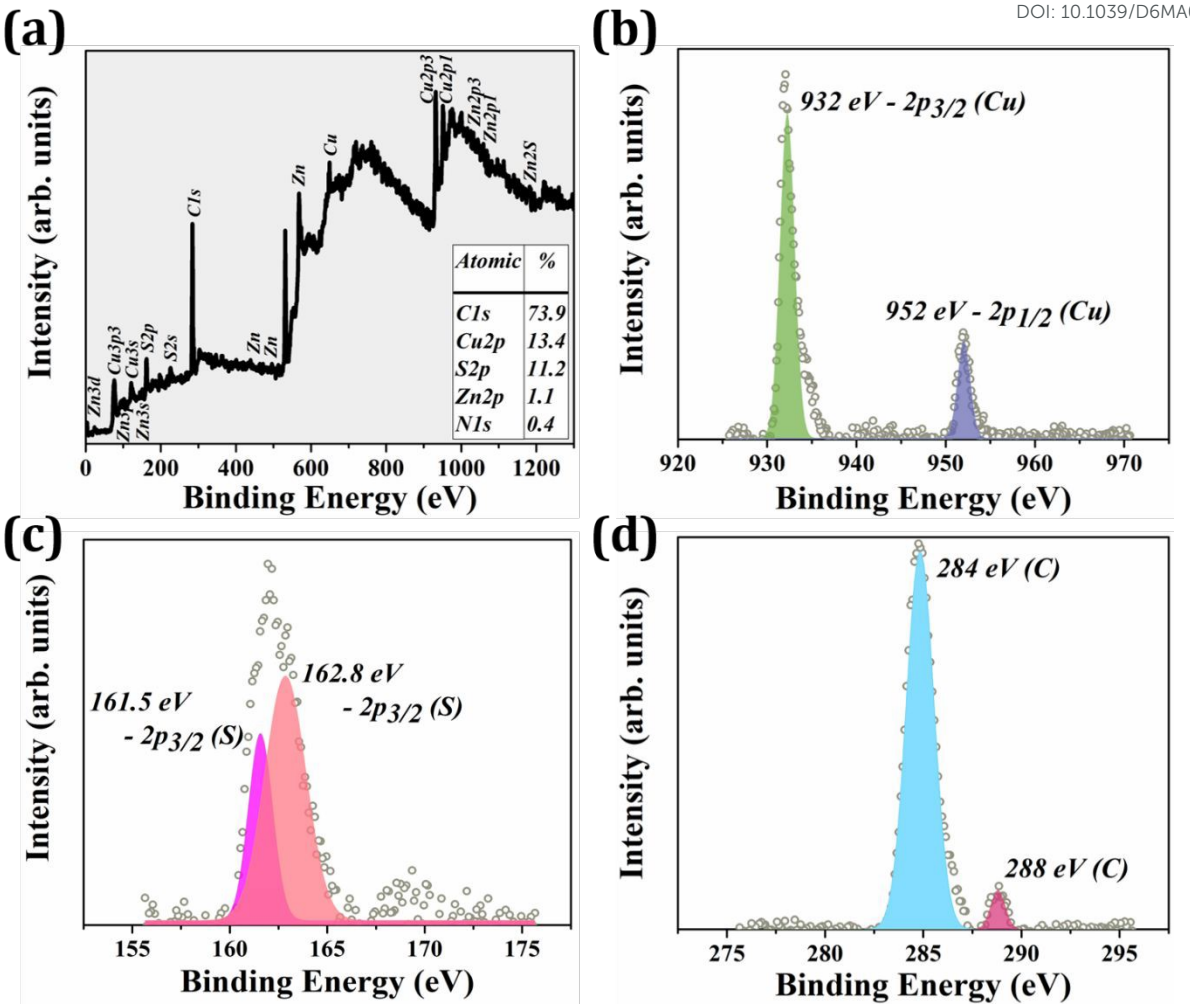

Figure 5: Surface chemical composition analysis by XPS. (a) Full survey spectrum of various elements presents in CZS composite. (b) Cu 2p high resolution spectra revealed multiple oxidation peaks corresponds to Cu $2p_{3/2}$ and Cu $2p_{1/2}$. (c) S 2p spectra revealed two different peaks at 161.5 and 162.8 eV confirms the divalent oxidation state of S $2p_{3/2}$. (d) C 1s element displayed two different peaks, attributes to C-C and C=O, respectively. The experimental results are represented by grey circles, and the bonds were validated for various values using the NIST-XPS database.

3.5 Surface area and angle

To know specific surface area and porosity of as-synthesized three photocatalysts are characterized by nitrogen adsorption-desorption isotherm as illustrated in **Figure 6**. As shown

Materials Advances Accepted Manuscript

View Article Online
DOI: 10.1039/D6MA00191B

Open Access Article. Published on 20 June 2026. Downloaded on 6/20/2026 11:52:44 PM.
This article is licensed under a Creative Commons Attribution-NonCommercial 3.0 Unported Licence.

in **Figure 6(a)**, the isotherms of ZnS, CuS and CZS heterojunction photocatalyst all exhibits typical type IV behaviour, as per IUPAC classification, indicative mesopores structure (pore diameters ranging from 2 to 50 nm). In addition, based on the shape of hysteresis loop it was confirmed that all three photocatalysts shows the H3 type, suggests the dominance of slit-like mesopores, generally associated with the aggregation of layered or plate-like particles. In particular ZnS, adsorption-desorption loop shows the capillary condensation at intermediate relative pressures (P/P_0), confirming the mesoporosity, whereas, though CuS retains mesoporosity, it has a higher degree of structural disorder or pore irregularity due to less defined hysteresis loop. But CZS photocatalyst shows improved mesoporosity due to nitrogen uptake and broader hysteresis loop, which attributed to the synergistic integration of both ZnS as well as CuS phases. All these results are well consistence with TEM analysis (**Figure 3**). The corresponding BJH (Barrett-Joyner-Halenda) pore size distribution analysis reveals the average pore diameters of 16.35 Å (ZnS), 16.54 Å (CuS), and 17.73 Å (CZS) as illustrated in **Figure 6(b)**. Additionally, calculated BET (Brunauer-Emmett-Teller) specific surface area and remaining textural values are listed in Table. A well-developed mesoporous structure plays a vital role in photocatalytic systems because it improves the diffusion and transport of reactant as well as product species within the material, while simultaneously allowing for better light harvesting due to the increased surface area and the internal light scattering.(38) The increased porosity found in the CZS composite can be due to the establishment of a heterojunction framework, which creates an interconnected pore architecture that not only improves mass transport but also ensures greater photocatalytic effectiveness.

In photocatalysis, a catalyst with high wettability has a major impact due to reactant adsorption. Thus, in addition to surface area, we measured contact angles to investigate the surface energy and wettability of all three photocatalysts. In general, contact angle measurement provides information about the surface wettability of the catalyst in terms of the

Materials Advances Accepted Manuscript

View Article Online
DOI: 10.1039/D6MA00191B

angle between the solid surface of the catalyst and a droplet of liquid (in this case, water). A catalyst with a high contact angle (>90°) is hydrophobic (low wettability), whereas a low contact angle (<90°) suggests hydrophilic (high wettability). **Figure 6(c)** demonstrates that bare ZnS and CuS have hydrophilic angles of 27.36° and 13.79°, respectively, whereas CZS heterojunction photocatalyst has a superhydrophilic angle of 7.32° (due to <10°). As a result of the synergistic phase integration (ZnS and CuS), the CZS photocatalyst exhibits optimum contact angle behaviour by potentially boosting the hydrophilic property, which considerably increases photocatalytic performance and evaluates a greater quantity of hydrogen.

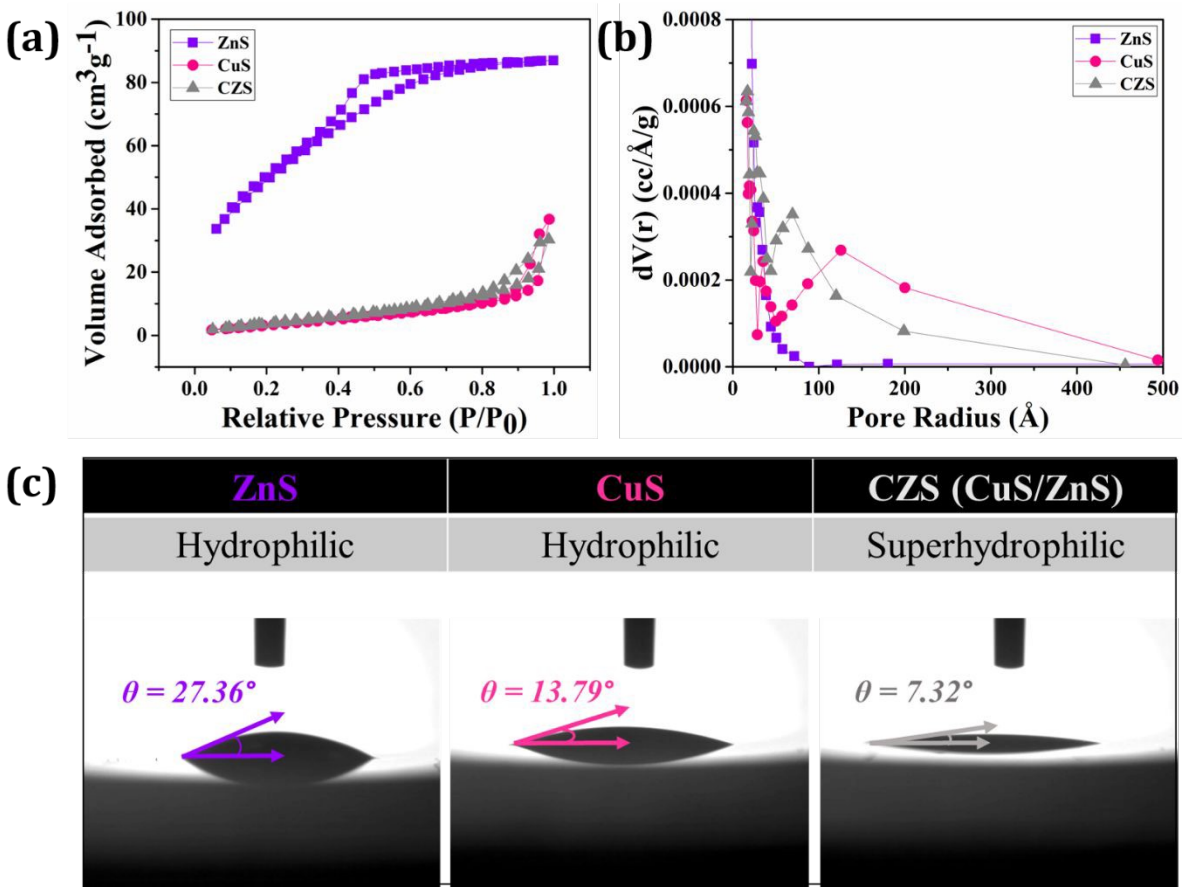

Figure 6: **Surface area and surface angle**. The bare ZnS (purple colour) and bare CuS (pink colour) were employed as controls for the CZS composite (grey colour). (a) Nitrogen adsorption-desorption isotherm (BET analysis); (b) BJH pore size distribution curve based on nitrogen adsorption-desorption isotherms. All photocatalysts exhibit an H3-hysteresis loop with a type IV isotherm and mesoporosity,

Open Access Article. Published on 20 June 2026. Downloaded on 6/20/2026 11:52:44 PM.
This article is licensed under a Creative Commons Attribution-NonCommercial 3.0 Unported Licence.

Materials Advances Accepted Manuscript

View Article Online
DOI: 10.1039/D6MA00191B

but CZS has a more pronounced distribution, which improves mass transfer and active site exposure during the photocatalytic process. (c) Static water contact angle measurement indicates hydrophilic (bare ZnS and CuS) and superhydrophilic (CZS) behaviour, showing an improvement in the interaction between photocatalyst and aqueous reactants, consequently impacting H_2 efficiency.

Open Access Article. Published on 20 June 2026. Downloaded on 6/20/2026 11:52:44 PM.
This article is licensed under a Creative Commons Attribution-NonCommercial 3.0 Unported Licence.

3.6 Hydrogen evolution analysis via photocatalytic water splitting

The photocatalytic water splitting experiment was performed on CZS composite in order to examine its catalytic efficiency in water splitting by using 0.1 M Na_2SO_4 as a sacrificial agent (electron donor). However, sacrificial agents play a critical role in increasing the overall efficiency of the photocatalyst by transferring the photo-electrons from photo-absorber to water molecule, thereby reducing water (H_2 evolution). A photo-chemical reactor was used to study the photocatalytic measurement as depicted in **Figure S5 (a)** and the amount of H_2 evolution was collected and analyzed by gas chromatogram (GC) as shown in **Figure S5 (b)**. The photocatalyst was illuminated by using solar simulator (the reactor setup was picturised in **Figure S5**) for 12 hours continuously and the redox measurements were collected at regular time interval (3 hours). **Figure 7** depicts the photocatalytic water splitting performance of three different catalysts such as bare ZnS, CuS and CZS composite and the H_2 evolution values are presented as cumulative production (μmol g^{-1}) and corresponding average rates (μmol g^{-1} h^{-1}) are calculated from time-dependent measurements. Firstly, as shown in **Figure 7(a)**, the bare ZnS photocatalyst was tested and the H_2 evolution was 2000 μmol g^{-1} after the illumination of light for 6 hours continuously, because it has the wide bandgap energy (3.3 eV), it cannot be active to absorb visible energy. Whereas, in case of bare CuS, it has the H_2 production of 4450 μmol g^{-1} (2.2 times higher than bare ZnS) due to its optical bandgap energy of 1.6 eV, which can absorb more visible light. But with the CZS composite photocatalyst showed enhanced H_2 production of 6000 μmol g^{-1} (3 times higher than bare ZnS) due to its wide optical band energy

Materials Advances Accepted Manuscript

View Article Online
DOI: 10.1039/D6MA00191B

gap ~1.4 eV. These results suggested that CZS composite exhibited higher green H_2 production and led to subsequent measurement. The same experiment was performed continuously for 12 hours at a regular time interval of time with CZS composite, as depicted in **Figure 7(c)**. According to the time-dependent study, it was observed that the cumulative H_2 evolution was hugely increased to 12,145 μmol g^{-1} at 12 hours continuous irradiation of light (corresponding to an average H_2 evolution rate ~1,012 μmol g^{-1} h^{-1}). This photocatalytic enhancement can be attributed to efficient interfacial charge separation between ZnS and CuS. Based on illumination, both semiconductors are photoexcited, generating electron-hole pairs. Both the semiconductors have a close interfacial contact and align their bands, which efficiently separates the photogenerated charge carrier. Based on the reported band structures of CuS and ZnS, charge transfer process is likely controlled by heterojunction mechanism, where the photogenerated electrons tend to migrate into CB of ZnS and holes accumulate in CuS.(38) This directed movement facilitates the spatial separation of charge carrier, allowing electrons to reduce adsorbed H^+ ions to H_2 while the solution species consumes the holes. Additionally, the production of CuS/Cu_2S species during the photocatalytic process may act as electron trapping sites and co-catalytic centres, enhancing the H_2 evolution reaction and promoting a charge separation. Compared to individual components, CZS composite has enhanced photocatalytic efficacy which supports the existence of effective interfacial charge transfer. The resulted enhancement may potentially be attributed to interfacial charge transfer (IFCT), in which photogenerated carriers migrate rapidly across the interface due to strong electronic coupling between both the semiconductors (CuS and ZnS). However, it should be noted that an alternative mechanism, such as a Z-scheme charge transfer pathway, cannot be ruled out based on the present data. Therefore, based on the nature of charge transfer pathway and current optical as well as photocatalytic data suggests the formation of heterojunction system, possibly consistent with Type-II charge transfer behaviour.

Open Access Article. Published on 20 June 2026. Downloaded on 6/20/2026 11:52:44 PM.
This article is licensed under a Creative Commons Attribution-NonCommercial 3.0 Unported Licence.

Materials Advances Accepted Manuscript

View Article Online
DOI: 10.1039/D6MA00191B

Open Access Article. Published on 20 June 2026. Downloaded on 6/20/2026 11:52:44 PM.
This article is licensed under a Creative Commons Attribution-NonCommercial 3.0 Unported Licence.

On the other hand, surface properties also influence the adsorption-desorption equilibrium and reaction kinetics, which are critical sustained photocatalytic performance. The formation of heterostructure surface is by the intimate contact between CuS and ZnS, which provides a large number of active sites for adsorption of reactant species, especially H^+ ions. In photocatalytic H_2 evolution, effective reactant adsorption on the catalyst surface is a critical step because it promotes subsequent reduction reactions. Also, separation and migration of photogenerated carriers can be facilitated by interfaces, heterojunction boundaries and surface defects functioning as active sites for charge transfer. The heterogenous and rough surface morphology of CZS composite increases the amount of accessible catalytic sites and surface area. Besides that, interfacial contact between CuS and ZnS improves the charge carrier movement across the surface, by reducing the recombination losses and enabling more efficient usage of photogenerated electrons for H_2 evolution. The additional surface-active sites and the co-catalytic centres could be provided by the potential production of CuS/Cu2S species, which would further enhance the reaction kinetics. Therefore, the higher photocatalytic efficacy of CZS nanocomposite is largely due to the combined effects of increased surface area, a large number of active sites and effective interfacial charge transfer. In addition to this, **Table 1** shows the list of various Zn and Cu based nanomaterials used for green H_2 evolution via PC and in contrast to the table, CZS photocatalyst gives the highest H_2 rate. In addition, the amount of H_2 evolution in ppm of three catalyst (ZnS, CuS and CZS) after the 6 hours illumination of photons were illustrated in **Figure S6 (a)** and the time-dependent study of CZS nanocomposite, measured at 0, 3, 6, 9 and 12 hours under continuous irradiation of photons was showed in **Figure S6 (b)**.

We also performed catalytic experiments using a physical mixture (Phy.Mix) of ZnS and CuS (in 1:1 ratio) at 9 hours illumination of solar, alongside the individual photocatalysts (ZnS, CuS and CZS). However, the H_2 efficiency of Phy.Mix was significantly lower compared

Materials Advances Accepted Manuscript

View Article Online
DOI: 10.1039/D6MA00191B

to the CZS heterojunction as shown in **Figure S7 (a)**. Furthermore, when CZS nanocomposite was subjected to continuous irradiation for 15 hours, a notable decline in H_2 evolution was observed **(Figure S8 (a))**. Post-photocatalysis morphological analysis of CZS nanocomposite (**Figure S8 (b))** shows the discernible structural changes compared to before photocatalysis sample. The particles appeared more dispersed and loosely packed, exhibiting magnified surface roughness along with the structure of small plate-like or flake-like characteristics. These morphological alterations indicated a partial structural degradation, likely caused by prolonged solar exposure, photo-corrosion and surface instability of catalyst. Initially dense clusters disintegrating demonstrated that the photocatalytic performance modifies the catalyst surface. Such surface modifications may reduce the number of active sites and contribute to the observed decline in H_2 evolution activity. Overall, while CZS nanocomposite retains its general structural framework, prolonged irradiation induces surface deterioration and increased particle dispersion, which are likely responsible for gradual decrease in photocatalytic performance. This kind of behaviour is commonly observed in metal sufide-based photocatalysts under prolonged illumination conditions. Despite this, the catalyst retains a significant portion of its activity, indicating reasonable operational stability over the tested timeframe. But to mitigate the photo-corrosion, the potential approaches such as, surface passivation or protective coatings, formation of more robust heterostructure or core-shell architectures, incorporation of other co-catalyst, usage of suitable hole scavengers and etc. might help to improve the long-term durability of the photocatalyst for practical applications.

TABLE 1: Table finds the amount of H_2 evolution rate via various Cu-based and Zn-based photocatalysts by using PC technique.

S.No	Catalyst	Synthesis Technique	Mediator	H_2 Evolution	Ref
1.	Cu_3P/S	Wet chemical	Na_2S/Na_2SO_3	2,085 μmol g^{-1} h^{-1}	(43)
2.	$Cu_3P/g\text{-}C_3N_4$	Chemical deposition and phosphorization	TEOA (10 vol%)	808 μmol g^{-1} h^{-1}	(44)

Open Access Article. Published on 20 June 2026. Downloaded on 6/20/2026 11:52:44 PM.
This article is licensed under a Creative Commons Attribution-NonCommercial 3.0 Unported Licence.

Materials Advances Accepted Manuscript

View Article Online
DOI: 10.1039/D6MA00191B

3.	CuS/TiO_2	Co-precipitation	Na_2S/Na_2SO_3	1262 μmol g^{-1} h^{-1}	(45)
4.	CuS/ZnS porous nanosheets	Hydrothermal and cation exchange reaction	Na_2S/Na_2SO_3	4147 μmol g^{-1} h^{-1}	(38)
5.	5%CuS/CdS mesoporous nanocrystals	Chemical ion-exchange process	Na_2S/Na_2SO_3	280 μmol g^{-1} h^{-1}	(46)
6.	Cu(0.05 wt%)-g-C_3N_4	In-situ reduction method	TEOA (10 vol%)	241.3 μmol g^{-1} h^{-1}	(47)
7.	ZnS/CuS nanotubes	Sulfuration and subsequent cation exchange reaction	Na_2S/Na_2SO_3	56.47 μmol g^{-1} h^{-1}	(48)
8.	CuS/g-C_3N_4	In-situ growth method	TEOA (10 vol%)	17.2 μmol g^{-1} h^{-1}	(49)
9.	TiO_2/CuO composite Nanofibers	Electrospinning	D.I water and methanol (9:1)	1146.9 μmol g^{-1} h^{-1}	(50)
10.	Cu/g-C3N4	Facile method	25% methyl alcohol	20.5 μmol g^{-1} h^{-1}	(51)
12.	CdS/g-C_3N_4/CuS	Novel and facile low-temperature solid-state method	Na_2S/Na_2SO_3	57.56 μmol g^{-1} h^{-1}	(52)
14.	$(Zn_{0.95}Cu_{0.05})_{1-x}$ Cd_xS (x = 0.33)	Simple co-precipitation	Na_2S/Na_2SO_3	508 μmol h^{-1}	(53)
15.	Cu doped ZnO	Co-precipitation	KOH (0.5M)	1931.8 μmol h^{-1}	(54)
16.	CuS/TiO_2	Hydrothermal method at high temperature	50% of methanol	570 μmol h^{-1}	(55)
17.	Ni:Cu_xS/EY	Facile colloidal	TEOA (10 vol%)	4000 μmol g^{-1} h^{-1}	(56)
18.	CuS/MXene	Wet-chemical	Na_2S/Na_2SO_3	4.245 μmol g^{-1} h^{-1}	(57)
19.	$MoS_2/CuInS_2$	Hydrothermal	Na_2S/Na_2SO_3	316 μmol g^{-1} h^{-1}	(58)
20.	g-C_3N_4–CuS	Hydrothermal	TEOA (10 vol%)	126.5 μmol h^{-1}	(59)
21.	$CuS/CdIn_2S_4/ZnIn_2S_4$	Microwave hydrothermal	Na_2S/Na_2SO_3	358.4 μmol g^{-1} h^{-1}	(60)
22.	Cu–S@MoS_2	Solvothermal	D.I water	9.86 μmol g^{-1} h^{-1}	(61)
23.	CuS/TiO_2	Co-precipitation	Methanol (20 vol%)	2.95 mmol g^{-1} h^{-1}	(62)
24.	Cu_7S_4 nanosheet decorated TiO_2	Coprecipitation	TEOA (10 vol%)	11.5 mmol g^{-1} h^{-1}	(63)
25.	ZnS–CuS–CdS	Collidal-coprecipitation	60 mM Na_2S	837.6 μmol g^{-1} h^{-1}	(64)
26.	TiO_2/CuO/Cu	Electrospinning	D.I water and methanol	851.3 μmol g^{-1} h^{-1}	(65)
27.	CdS/CdSe/CuS hollow nanospheres	Vulcanization and selenization	Na_2S/Na_2SO_3	723 μmol h^{-1}	(66)

Open Access Article. Published on 20 June 2026. Downloaded on 6/20/2026 11:52:44 PM.
This article is licensed under a Creative Commons Attribution-NonCommercial 3.0 Unported Licence.

Materials Advances Accepted Manuscript

28.	**CZS heterojunction**	**Hydrothermal**	**Na_2SO_4**	**12145 µmol g^{-1}**	**This Work**

View Article Online
DOI: 10.1039/D0MA00191B

Solar-to-hydrogen conversion efficiency (ηSTH) evaluates a photocatalyst's ability to produce H_2, comparing it to other photoactive materials and their efficiency in water splitting. One of the most important characteristics in the real-world application of overall water splitting *via* PC for solar H_2 production is STH, which means the ratio of solar energy preserved as a H_2 to incident solar energy. As reported in recent reviews, we followed the conventional way for measuring the photocatalytic activity, as well as STH efficiency calculations by following the equation (5).(67) **Figure 7(b) and 7(d)** demonstrates the calculated STH efficiency of bare ZnS was 0.03 % and CuS was 0.06 %, whereas, for CZS composite the efficiency showed 0.08 at 6 hours irradiation light and at 12 hours it was 0.16%. Therefore, due to the strong optical absorption property of CZS composite photocatalyst exhibited better H_2 conversion efficiency in comparison with bare photocatalyst. Therefore, these highly efficient photocatalysts are critically needed for sustainable energy generation and harvesting applications to meet the growing demands of society.

$$\eta_{STH} = \frac{\textbf{Out put energy as } H_2}{\textbf{Energy of incident solar light}} = \frac{r_{H_2} \times \Delta G_r}{P_{sun} \times S} \quad \textbf{(5)}$$

** P_{sun} - energy flux of sunlight, S - irradiated area, r_{H2} - H_2 production rate, and ΔGr - reaction Gibbs energy.*

Open Access Article. Published on 20 June 2026. Downloaded on 6/20/2026 11:52:44 PM.
This article is licensed under a Creative Commons Attribution-NonCommercial 3.0 Unported Licence.

Materials Advances Accepted Manuscript

View Article Online
DOI: 10.1039/D6MA00191B

Open Access Article. Published on 20 June 2026. Downloaded on 6/20/2026 11:52:44 PM.
This article is licensed under a Creative Commons Attribution-NonCommercial 3.0 Unported Licence.

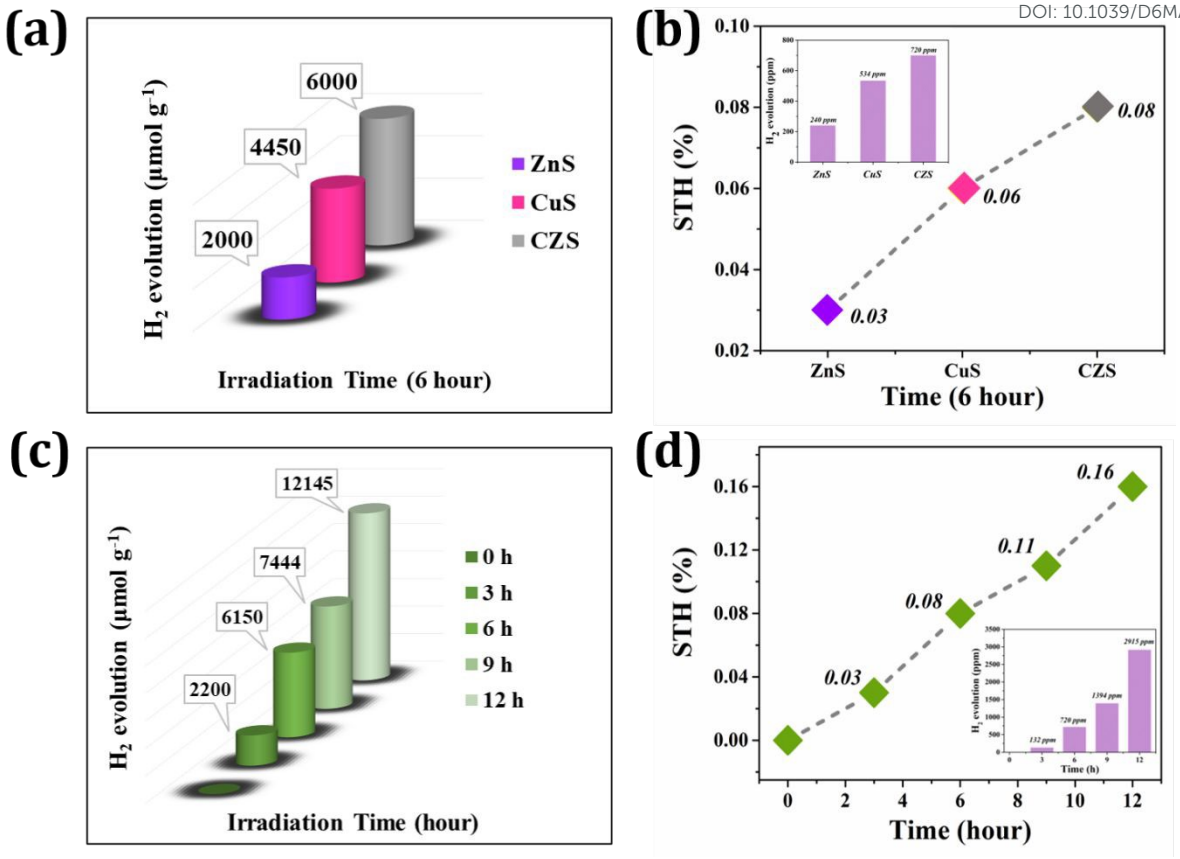

Figure 7: **Photocatalytic H_2 evolution measurement**. (a) H_2 evolution analysis of three different photocatalysts after 6 hours of solar light irradiation: bare ZnS (purple colour), bare CuS (pink colour) and CZS composite (grey colour) exhibited better H_2 production rate than controls. (b) STH% of bare ZnS was 0.03%, CuS was 0.06% and CZS composite results 0.08%. (c) The time-dependent cumulative H_2 evolution of CZS composite under solar light illumination, reaching 12,145 µmol g^{-1} after 12 hours. (d) The respective STH% for CZS photocatalyst is ~0.16% at 12 hours illumination of light.

4. Conclusion

CuS/ZnS (CZS) hetero-structured photocatalyst greatly enhances the photocatalytic H2 evolution performance, overcoming the limitations of pristine CuS and ZnS photocatalysts. The effective charge separation created by intimate contact between the semiconductors of CuS and ZnS, which promotes directed migration of the photogenerated charge carries and prevents

Materials Advances Accepted Manuscript

View Article Online
DOI: 10.1039/D6MA00191B

the electron-hole recombination, is the cause of this improvement. The charge transfer behaviour is consistent with a heterojunction process and possibly resembling Type-II band alignment. Under continuous irradiation of 1-sun, CZS composite achieved an impressive cumulative H_2 evolution production of 12,145 μmol g^{-1} after 12 hours, along with STH efficiency of ~0.16%, demonstrating a significantly improved photocatalytic activity relative to pristine photocatalysts. Additionally, the enhanced performance is supported by synergistic physicochemical characteristics, including improved light absorption, a strong interfacial coupling, and a charge transfer dynamic arising from the hetero-structured system. However, a slow decrease in activity under the prolonged irradiation suggests the existence of effects related to photo-corrosion, indicating the necessity of additional tuning to enhance long-term stability. Despite this drawback, CZS system is a viable candidate for solar-driven H_2 generation due to its facile, low-temperature hydrothermal synthesis and use of relatively abundant materials. All these considerations, the present work offers the insightful information about the role of interfacial engineering which improves the photocatalytic performance and also suggests a possible route for fabrication of effective and scalable photocatalysts of sustainable H_2.

5. Conflict of Interests

No conflicts to disclose from all the authors.

6. Authors Contribution

Conceptualization, G.K.D., and S.C.; methodology, A.M.S.K.; writing - original draft, A.M.S.K., K.B.B., S.C. and G.K.D.; characterization, A.M.S.K., and K.B.B.; review and editing, K.B.B., S.C. and G.K.D.; supervision, G.K.D., and S.C.; project administration, G.K.D.; data curation, A.M.S.K., S.C. and G.K.D. All authors have read and agreed to the published version of the manuscript.

Open Access Article. Published on 20 June 2026. Downloaded on 6/20/2026 11:52:44 PM.
This article is licensed under a Creative Commons Attribution-NonCommercial 3.0 Unported Licence.

Materials Advances Accepted Manuscript

View Article Online
DOI: 10.1039/D6MA00191B

7. Data Availability Statement

The data that supports these findings of the study are available from the corresponding author upon reasonable request.

8. Acknowledgements

A.M.S.K. would like to thank SRM University and AP their financial support. Dr. Sabyasachi Chakrabortty acknowledges the financial support from Anusandhan National Research Foundation (ANRF) under Science & Engineering Research Board (SERB) State University Research Excellence (SERB SURE) Scheme (SUR/2022/001424), DST-FIST (SR-FST-CS-I-2021-219(C)) and SRM University AP, Andhra Pradesh for internal research grant (SRMAP/URG/General-D/2025-26/012). We acknowledge the Nanotechnology Research Centre (NRC), and SCIF:SRM Central Instrumentation Facility, SRMIST for providing the research facilities.

9. References

1. Zou X, Zhang Y. Noble metal-free hydrogen evolution catalysts for water splitting. Chem Soc Rev [Internet]. 2015;44(15):5148–80. Available from: http://dx.doi.org/10.1039/C4CS00448E
2. Chatterjee P, Ambati MSK, Chakraborty AK, Chakrabortty S, Biring S, Ramakrishna S, et al. Photovoltaic/photo-electrocatalysis integration for green hydrogen: A review. Energy Convers Manag [Internet]. 2022;261(April):115648. Available from: https://doi.org/10.1016/j.enconman.2022.115648
3. Liu F, Shi C, Guo X, He Z, Pan L, Huang ZF, et al. Rational Design of Better Hydrogen Evolution Electrocatalysts for Water Splitting: A Review. Adv Sci [Internet]. 2022 Jun 1;9(18):2200307. Available from: https://doi.org/10.1002/advs.202200307
4. Kochuveedu ST. Photocatalytic and Photoelectrochemical Water Splitting on TiO2 via

Open Access Article. Published on 20 June 2026. Downloaded on 6/20/2026 11:52:44 PM.
This article is licensed under a Creative Commons Attribution-NonCommercial 3.0 Unported Licence.

Materials Advances Accepted Manuscript

View Article Online
DOI: 10.1039/D6MA00191B

Photosensitization. J Nanomater [Internet]. 2016 Jan 1;2016(1):4073142. Available from: https://doi.org/10.1155/2016/4073142

5. Qureshi F, Tahir M. Photoelectrochemical water splitting with engineering aspects for hydrogen production: Recent advances, strategies and challenges. Int J Hydrogen Energy [Internet]. 2024;69:760–76. Available from: https://www.sciencedirect.com/science/article/pii/S0360319924017269
6. Song H, Luo S, Huang H, Deng B, Ye J. Solar-Driven Hydrogen Production: Recent Advances, Challenges, and Future Perspectives. ACS Energy Lett [Internet]. 2022 Mar 11;7(3):1043–65. Available from: https://doi.org/10.1021/acsenergylett.1c02591
7. Kannan K, Gautam J, Chanda D, Meshesha MM, Jang SG, Yang BL. Two dimensional MAX supported copper oxide/nickel Oxide/MAX as an efficient and novel photocatalyst for hydrogen evolution. Int J Hydrogen Energy [Internet]. 2023;48(20):7273–83. Available from: https://www.sciencedirect.com/science/article/pii/S036031992204825X
8. Kannan K, Chanda D, Gautam J, Behera A, Meshesha MM, Gwon Jang S, et al. Hydrothermally synthesized mixed metal oxide nanocomposites for electrochemical water splitting and photocatalytic hydrogen production. Int J Hydrogen Energy [Internet]. 2023;48(93):36412–26. Available from: https://www.sciencedirect.com/science/article/pii/S0360319923028550
9. Mekete Meshesha M, Gautam J, Chanda D, Kannan K, Gwon Jang S, Lyong Yang B. Effect of reaction temperature on morphology and photoelectrochemical performance of titanium dioxide. Mater Lett [Internet]. 2022;329:133176. Available from: https://www.sciencedirect.com/science/article/pii/S0167577X22015312
10. Meshesha MM, Kannan K, Chanda D, Gautam J, Jang SG, Yang BL. Remarkable photoelectrochemical activity of titanium dioxide nanorod arrays sensitized with

Open Access Article. Published on 20 June 2026. Downloaded on 6/20/2026 11:52:44 PM.
This article is licensed under a Creative Commons Attribution-NonCommercial 3.0 Unported Licence.

Materials Advances Accepted Manuscript

View Article Online
DOI: 10.1039/D6MA00191B

transition metal sulfide nanoparticles for solar hydrogen production. Mater Today Chem [Internet]. 2022;26:101216. Available from: https://www.sciencedirect.com/science/article/pii/S2468519422004451

11. Wang L, Yu J. Chapter 1 - Principles of photocatalysis. In: Yu J, Zhang L, Wang L, Zhu BBTIS and T, editors. S-scheme Heterojunction Photocatalysts [Internet]. Elsevier; 2023. p. 1–52. Available from: https://www.sciencedirect.com/science/article/pii/B9780443187865000020
12. Yang X, Wang D. Photocatalysis: From Fundamental Principles to Materials and Applications. ACS Appl Energy Mater [Internet]. 2018 Dec 24;1(12):6657–93. Available from: https://doi.org/10.1021/acsaem.8b01345
13. Wang P, Liu Z, Han C, Ma X, Tong Z, Tan B. Cu2O/CuO heterojunction formed by thermal oxidation and decorated with Pt co-catalyst as an efficient photocathode for photoelectrochemical water splitting. J Nanoparticle Res [Internet]. 2021;23(12):268. Available from: https://doi.org/10.1007/s11051-021-05383-2
14. Cai Q, Liu Z, Han C, Tong Z, Ma C. CuInS2/Sb2S3 heterostructure modified with noble metal co-catalyst for efficient photoelectrochemical water splitting. J Alloys Compd [Internet]. 2019;795:319–26. Available from: https://www.sciencedirect.com/science/article/pii/S0925838819316184
15. Jia T, Ruan M, Li G, Michorczyk P, Wang C, Liu Z. Ca2+ substitution induced phase coexistence and synergistic regulation of Ti3+ defects to improve piezoelectric–photocatalytic water splitting performance of BaTiO3. J Mater Chem A [Internet]. 2026;14(3):1908–22. Available from: http://dx.doi.org/10.1039/D5TA08280C
16. Iwashina K, Iwase A, Ng YH, Amal R, Kudo A. Z-Schematic Water Splitting into H2 and O2 Using Metal Sulfide as a Hydrogen-Evolving Photocatalyst and Reduced Graphene Oxide as a Solid-State Electron Mediator. J Am Chem Soc [Internet]. 2015

Open Access Article. Published on 20 June 2026. Downloaded on 6/20/2026 11:52:44 PM.
This article is licensed under a Creative Commons Attribution-NonCommercial 3.0 Unported Licence.

Materials Advances Accepted Manuscript

Jan 21;137(2):604–7. Available from: https://doi.org/10.1021/ja511615s
View Article Online
DOI: 10.1039/D6MA00191B

17. Chen X, Ruan M, Wang C, Zhong T, Liu Z. Phase engineering to construct In2S3 heterophase junctions and abundant active boundaries and surfaces for efficient Pyro-PEC performance in CdS/In2S3. J Mater Chem A [Internet]. 2024;12(25):15440–52. Available from: http://dx.doi.org/10.1039/D4TA01455C

18. Chen X, Shen S, Guo L, Mao SS. Semiconductor-based Photocatalytic Hydrogen Generation. Chem Rev [Internet]. 2010 Nov 10;110(11):6503–70. Available from: https://doi.org/10.1021/cr1001645

19. Hao X, Wang Y, Zhou J, Cui Z, Wang Y, Zou Z. Zinc vacancy-promoted photocatalytic activity and photostability of ZnS for efficient visible-light-driven hydrogen evolution. Appl Catal B Environ [Internet]. 2018;221:302–11. Available from: https://www.sciencedirect.com/science/article/pii/S0926337317308317

20. Wang G, Huang B, Li Z, Lou Z, Wang Z, Dai Y, et al. Synthesis and characterization of ZnS with controlled amount of S vacancies for photocatalytic H2 production under visible light. Sci Rep [Internet]. 2015;5(1):8544. Available from: https://doi.org/10.1038/srep08544

21. Xu L, Ao Y, Guan B, Xiang Y, Guan J. Coordination Complex Transformation-Assisted Fabrication for Hollow Chestnut-Like Hierarchical ZnS with Enhanced Photocatalytic Hydrogen Evolution. Vol. 9, Nanomaterials. 2019.

22. Lo SS, Mirkovic T, Chuang CH, Burda C, Scholes GD. Emergent Properties Resulting from Type-II Band Alignment in Semiconductor Nanoheterostructures. Adv Mater [Internet]. 2011 Jan 11;23(2):180–97. Available from: https://doi.org/10.1002/adma.201002290

23. Soltani N, Saion E, Yunus WMM, Erfani M, Navasery M, Bahmanrokh G, et al. Enhancement of visible light photocatalytic activity of ZnS and CdS nanoparticles based

Open Access Article. Published on 20 June 2026. Downloaded on 6/20/2026 11:52:44 PM.
This article is licensed under a Creative Commons Attribution-NonCommercial 3.0 Unported Licence.

Materials Advances Accepted Manuscript

View Article Online
DOI: 10.1039/D0MA00191B

on organic and inorganic coating. Appl Surf Sci [Internet]. 2014;290:440–7. Available from: https://www.sciencedirect.com/science/article/pii/S016943321302182X

24. Zhang Y, Tian J, Li H, Wang L, Qin X, Asiri AM, et al. Biomolecule-Assisted, Environmentally Friendly, One-Pot Synthesis of CuS/Reduced Graphene Oxide Nanocomposites with Enhanced Photocatalytic Performance. Langmuir [Internet]. 2012 Sep 4;28(35):12893–900. Available from: https://doi.org/10.1021/la303049w

25. Basu M, Sinha AK, Pradhan M, Sarkar S, Negishi Y, Pal T. Evolution of Hierarchical Hexagonal Stacked Plates of CuS from Liquid−Liquid Interface and its Photocatalytic Application for Oxidative Degradation of Different Dyes under Indoor Lighting. Environ Sci Technol [Internet]. 2010 Aug 15;44(16):6313–8. Available from: https://doi.org/10.1021/es101323w

26. Liu Y, Liu M, Swihart MT. Plasmonic Copper Sulfide-Based Materials: A Brief Introduction to Their Synthesis, Doping, Alloying, and Applications. J Phys Chem C [Internet]. 2017 Jun 29;121(25):13435–47. Available from: https://doi.org/10.1021/acs.jpcc.7b00894

27. Yendrapati TP, Gautam A, Bojja S, Pal U. Formation of ZnO@CuS nanorods for efficient photocatalytic hydrogen generation. Sol Energy [Internet]. 2020;196:540–8. Available from: https://www.sciencedirect.com/science/article/pii/S0038092X1931268X

28. Friedrich D, Schlosser M, Pfitzner A. Interconversion of One-Dimensional Thiogallates Cs2[Ga2(S2)2–xS2+x] (x = 0, 1, 2) by Using High-Temperature Decomposition and Polysulfide-Flux Reactions. Cryst Growth Des [Internet]. 2017 Sep 6;17(9):4887–92. Available from: https://doi.org/10.1021/acs.cgd.7b00840

29. Quan Z, Wang Y, Fang J. High-Index Faceted Noble Metal Nanocrystals. Acc Chem Res [Internet]. 2013 Feb 19;46(2):191–202. Available from:

Open Access Article. Published on 20 June 2026. Downloaded on 6/20/2026 11:52:44 PM.
This article is licensed under a Creative Commons Attribution-NonCommercial 3.0 Unported Licence.

Materials Advances Accepted Manuscript

View Article Online
DOI: 10.1039/D6MA00191B

https://doi.org/10.1021/ar200293n

30. Im MH, Kim YJ. Energy transfer and multiple photoluminescence of LuNbO4 co-doped with Eu3+ and Tb3+. Mater Res Bull [Internet]. 2019;112:399–405. Available from: https://www.sciencedirect.com/science/article/pii/S0025540818329623

31. Perng DC, Hong MH, Chen KH, Chen KH. Enhancement of short-circuit current density in Cu2O/ZnO heterojunction solar cells. J Alloys Compd [Internet]. 2017;695:549–54. Available from: https://www.sciencedirect.com/science/article/pii/S092583881633585X

32. Béchu S, Ralaiarisoa M, Etcheberry A, Schulz P. Photoemission Spectroscopy Characterization of Halide Perovskites. Adv Energy Mater [Internet]. 2020 Jul 1;10(26):1904007. Available from: https://doi.org/10.1002/aenm.201904007

33. Wu C, Yu SH, Chen S, Liu G, Liu B. Large scale synthesis of uniform CuS nanotubes in ethylene glycol by a sacrificial templating method under mild conditions. J Mater Chem [Internet]. 2006;16(32):3326–31. Available from: http://dx.doi.org/10.1039/B606226A

34. Li B, Xie Y, Xue Y. Controllable Synthesis of CuS Nanostructures from Self-Assembled Precursors with Biomolecule Assistance. J Phys Chem C [Internet]. 2007 Aug 1;111(33):12181–7. Available from: https://doi.org/10.1021/jp070861v

35. Chen LY, Zhang YG, Wang WZ, Zhang ZD. Tunable Synthesis of Various Hierarchical Structures of In(OH)3 and In2O3 Assembled by Nanocubes. Eur J Inorg Chem [Internet]. 2008 Mar 1;2008(9):1445–51. Available from: https://doi.org/10.1002/ejic.200700936

36. Chen LY, Zhang ZD. Biomolecule-Assisted Synthesis of In(OH)3 Hollow Spherical Nanostructures Constructed with Well-Aligned Nanocubes and Their Conversion into C−In2O3. J Phys Chem C [Internet]. 2008 Dec 4;112(48):18798–803. Available from:

Open Access Article. Published on 20 June 2026. Downloaded on 6/20/2026 11:52:44 PM.
This article is licensed under a Creative Commons Attribution-NonCommercial 3.0 Unported Licence.

Materials Advances Accepted Manuscript

View Article Online
DOI: 10.1039/D6MA00191B

https://doi.org/10.1021/jp806100k

37. Wang X, Li Y, Wang M, Li W, Chen M, Zhao Y. Synthesis of tunable ZnS–CuS microspheres and visible-light photoactivity for rhodamine B. New J Chem [Internet]. 2014;38(9):4182–9. Available from: http://dx.doi.org/10.1039/C4NJ00264D

38. Zhang J, Yu J, Zhang Y, Li Q, Gong JR. Visible Light Photocatalytic H2-Production Activity of CuS/ZnS Porous Nanosheets Based on Photoinduced Interfacial Charge Transfer. Nano Lett [Internet]. 2011 Nov 9;11(11):4774–9. Available from: https://doi.org/10.1021/nl202587b

39. Zhang Y, Chang G, Liu S, Tian J, Wang L, Lu W, et al. Microwave-assisted, environmentally friendly, one-pot preparation of Pd nanoparticles/graphene nanocomposites and their application in electrocatalytic oxidation of methanol. Catal Sci Technol [Internet]. 2011;1(9):1636–40. Available from: http://dx.doi.org/10.1039/C1CY00296A

40. Chabalala MP, Matthews T, Mbokazi SP, Mugadza K, Bellamkonda S, Mamlouk M, et al. Iron Oxide-Carbon Black Promotional Effect on Palladium Nanoparticles Toward Ethylene Glycol Oxidation in Alkaline Medium: Experimental and Computational Studies. Energy Technol [Internet]. 2024 Feb 1;12(2):2300856. Available from: https://doi.org/10.1002/ente.202300856

41. Cai W, Shi Y, Zhao Y, Chen M, Zhong Q, Bu Y. The solvent-driven formation of multi-morphological Ag–CeO2 plasmonic photocatalysts with enhanced visible-light photocatalytic reduction of CO2. RSC Adv [Internet]. 2018;8(71):40731–9. Available from: http://dx.doi.org/10.1039/C8RA08938H

42. Wang Y, Jin Y, Jia M, Ruan H, Tao X, Liu X, et al. Enhanced Visible-Light Photocatalytic Activities of CeVO4-V2O3 Composite: Effect of Ethylene Glycol. Vol. 13, Catalysts. 2023.

Open Access Article. Published on 20 June 2026. Downloaded on 6/20/2026 11:52:44 PM.
This article is licensed under a Creative Commons Attribution-NonCommercial 3.0 Unported Licence.

Materials Advances Accepted Manuscript

View Article Online
DOI: 10.1039/D6MA00191B

43. Zhang X, Min KA, Zheng W, Hwang J, Han B, Lee LYS. Copper phosphosulfides as a highly active and stable photocatalyst for hydrogen evolution reaction. Appl Catal B Environ [Internet]. 2020;273:118927. Available from: https://www.sciencedirect.com/science/article/pii/S0926337320303428

44. Hua S, Qu D, An L, Jiang W, Wen Y, Wang X, et al. Highly efficient p-type Cu3P/n-type g-C3N4 photocatalyst through Z-scheme charge transfer route. Appl Catal B Environ [Internet]. 2019;240:253–61. Available from: https://www.sciencedirect.com/science/article/pii/S0926337318308403

45. Chandra M, Bhunia K, Pradhan D. Controlled Synthesis of CuS/TiO2 Heterostructured Nanocomposites for Enhanced Photocatalytic Hydrogen Generation through Water Splitting. Inorg Chem [Internet]. 2018 Apr 16;57(8):4524–33. Available from: https://doi.org/10.1021/acs.inorgchem.8b00283

46. Vamvasakis I, Trapali A, Miao J, Liu B, Armatas GS. Enhanced visible-light photocatalytic hydrogen production activity of three-dimensional mesoporous p-CuS/n-CdS nanocrystal assemblies. Inorg Chem Front [Internet]. 2017;4(3):433–41. Available from: http://dx.doi.org/10.1039/C6QI00515B

47. Chen J, Shen S, Guo P, Wang M, Wu P, Wang X, et al. In-situ reduction synthesis of nano-sized Cu2O particles modifying g-C3N4 for enhanced photocatalytic hydrogen production. Appl Catal B Environ [Internet]. 2014;152–153:335–41. Available from: https://www.sciencedirect.com/science/article/pii/S0926337314000678

48. Shao YB, Wang LH, Huang JH. ZnS/CuS nanotubes for visible light-driven photocatalytic hydrogen generation. RSC Adv [Internet]. 2016;6(87):84493–9. Available from: http://dx.doi.org/10.1039/C6RA17046C

49. Chen T, Song C, Fan M, Hong Y, Hu B, Yu L, et al. In-situ fabrication of CuS/g-C3N4 nanocomposites with enhanced photocatalytic H2-production activity via photoinduced

Open Access Article. Published on 20 June 2026. Downloaded on 6/20/2026 11:52:44 PM.
This article is licensed under a Creative Commons Attribution-NonCommercial 3.0 Unported Licence.

Materials Advances Accepted Manuscript

View Article Online
DOI: 10.1039/D0MA00191B

interfacial charge transfer. Int J Hydrogen Energy [Internet]. 2017;42(17):12210–9. Available from: https://www.sciencedirect.com/science/article/pii/S036031991731234X

50. Zhu L, Hong M, Ho GW. Fabrication of wheat grain textured TiO2/CuO composite nanofibers for enhanced solar H2 generation and degradation performance. Nano Energy [Internet]. 2015;11:28–37. Available from: https://www.sciencedirect.com/science/article/pii/S2211285514200747

51. Fan M, Song C, Chen T, Yan X, Xu D, Gu W, et al. Visible-light-drived high photocatalytic activities of Cu/g-C3N4 photocatalysts for hydrogen production. RSC Adv [Internet]. 2016;6(41):34633–40. Available from: http://dx.doi.org/10.1039/C5RA27755H

52. Cheng F, Yin H, Xiang Q. Low-temperature solid-state preparation of ternary CdS/g-C3N4/CuS nanocomposites for enhanced visible-light photocatalytic H2-production activity. Appl Surf Sci [Internet]. 2017;391:432–9. Available from: https://www.sciencedirect.com/science/article/pii/S0169433216313988

53. Zhang W, Zhong Z, Wang Y, Xu R. Doped Solid Solution: (Zn0.95Cu0.05)1−xCdxS Nanocrystals with High Activity for H2 Evolution from Aqueous Solutions under Visible Light. J Phys Chem C [Internet]. 2008 Nov 13;112(45):17635–42. Available from: https://doi.org/10.1021/jp8059008

54. Kanade KG, Kale BB, Baeg JO, Lee SM, Lee CW, Moon SJ, et al. Self-assembled aligned Cu doped ZnO nanoparticles for photocatalytic hydrogen production under visible light irradiation. Mater Chem Phys [Internet]. 2007;102(1):98–104. Available from: https://www.sciencedirect.com/science/article/pii/S0254058406002902

55. Wang Q, An N, Bai Y, Hang H, Li J, Lu X, et al. High photocatalytic hydrogen production from methanol aqueous solution using the photocatalysts CuS/TiO2. Int J

Open Access Article. Published on 20 June 2026. Downloaded on 6/20/2026 11:52:44 PM.
This article is licensed under a Creative Commons Attribution-NonCommercial 3.0 Unported Licence.

Materials Advances Accepted Manuscript

View Article Online
DOI: 10.1039/D6MA00191B

Hydrogen Energy [Internet]. 2013;38(25):10739–45. Available from: https://www.sciencedirect.com/science/article/pii/S036031991300565X

56. Sarilmaz A, Yanalak G, Aslan E, Ozel F, Patir IH, Ersoz M. Shape-controlled synthesis of copper based multinary sulfide catalysts for enhanced photocatalytic hydrogen evolution. Renew Energy [Internet]. 2021;164:254–9. Available from: https://www.sciencedirect.com/science/article/pii/S0960148120314725

57. Xie Y, Rahman MM, Kareem S, Dong H, Qiao F, Xiong W, et al. Facile synthesis of CuS/MXene nanocomposites for efficient photocatalytic hydrogen generation. CrystEngComm [Internet]. 2020;22(11):2060–6. Available from: http://dx.doi.org/10.1039/D0CE00104J

58. Yuan YJ, Chen DQ, Huang YW, Yu ZT, Zhong JS, Chen TT, et al. MoS2 Nanosheet-Modified CuInS2 Photocatalyst for Visible-Light-Driven Hydrogen Production from Water. ChemSusChem [Internet]. 2016 May 10;9(9):1003–9. Available from: https://doi.org/10.1002/cssc.201600006

59. Yu S, Webster RD, Zhou Y, Yan X. Ultrathin g-C3N4 nanosheets with hexagonal CuS nanoplates as a novel composite photocatalyst under solar light irradiation for H2 production. Catal Sci Technol [Internet]. 2017;7(10):2050–6. Available from: http://dx.doi.org/10.1039/C7CY00110J

60. Chen X, Li L, Zhang W, Li Y, Song Q, Dong L. Fabricate Globular Flower-like CuS/CdIn2S4/ZnIn2S4 with High Visible Light Response via Microwave-assisted One–step Method and Its Multipathway Photoelectron Migration Properties for Hydrogen Evolution and Pollutant Degradation. ACS Sustain Chem Eng [Internet]. 2016 Dec 5;4(12):6680–8. Available from: https://doi.org/10.1021/acssuschemeng.6b01543

61. Temerov F, Greco R, Celis J, Eslava S, Wang W, Yamamoto T, et al. Activating 2D MoS2 by loading 2D Cu–S nanoplatelets for improved visible light photocatalytic

Open Access Article. Published on 20 June 2026. Downloaded on 6/20/2026 11:52:44 PM.
This article is licensed under a Creative Commons Attribution-NonCommercial 3.0 Unported Licence.

Materials Advances Accepted Manuscript

View Article Online
DOI: 10.1039/D5MA00191B

hydrogen evolution, drug degradation, and CO2 reduction. Results Mater [Internet]. 2024;22:100569. Available from: https://www.sciencedirect.com/science/article/pii/S2590048X24000438

62. El-Gendy RA, El-Bery HM, Farrag M, Fouad DM. Metal chalcogenides (CuS or MoS2)-modified TiO2 as highly efficient bifunctional photocatalyst nanocomposites for green H2 generation and dye degradation. Sci Rep [Internet]. 2023;13(1):7994. Available from: https://doi.org/10.1038/s41598-023-34743-2

63. Liu W, Peng H, Li L, Wang M, Geng H, Huang X. Modulate the electronic structure of Cu7S4 nanosheet on TiO2 for enhanced photocatalytic hydrogen evolution. Nano Res [Internet]. 2023;16(4):4488–93. Available from: https://doi.org/10.1007/s12274-022-5169-6

64. Hong E, Kim D, Kim JH. Heterostructured metal sulfide (ZnS–CuS–CdS) photocatalyst for high electron utilization in hydrogen production from solar water splitting. J Ind Eng Chem [Internet]. 2014;20(5):3869–74. Available from: https://www.sciencedirect.com/science/article/pii/S1226086X14000185

65. Hou H, Shang M, Gao F, Wang L, Liu Q, Zheng J, et al. Highly Efficient Photocatalytic Hydrogen Evolution in Ternary Hybrid TiO2/CuO/Cu Thoroughly Mesoporous Nanofibers. ACS Appl Mater Interfaces [Internet]. 2016 Aug 10;8(31):20128–37. Available from: https://doi.org/10.1021/acsami.6b06644

66. Sun G, Shi JW, Zou Y, Mao S, Ma D, Lv Y, et al. One-step synthesis of CdS/CdSe/CuS hollow nanospheres in aqueous solution for enhanced photocatalytic hydrogen evolution. Sustain Energy Fuels [Internet]. 2020;4(7):3467–76. Available from: http://dx.doi.org/10.1039/D0SE00249F

67. Majji M, Abzal SM, Jacob N, Maiti P, Choppella S, Ravva MK, et al. Efficient photocatalytic green hydrogen production using crystalline elemental Boron

Open Access Article. Published on 20 June 2026. Downloaded on 6/20/2026 11:52:44 PM.
This article is licensed under a Creative Commons Attribution-NonCommercial 3.0 Unported Licence.

Materials Advances Accepted Manuscript

nanostructures under visible light. Int J Hydrogen Energy [Internet]. 2024;56:338–47. Available from: https://www.sciencedirect.com/science/article/pii/S0360319923064133

View Article Online
DOI: 10.1039/D6MA00191B

Open Access Article. Published on 20 June 2026. Downloaded on 6/20/2026 11:52:44 PM.
This article is licensed under a Creative Commons Attribution-NonCommercial 3.0 Unported Licence.

Materials Advances Accepted Manuscript

View Article Online
DOI: 10.1039/D6MA00191B

Data Availability

The data supporting this article has been included as part of the Supplementary Information.

Open Access Article. Published on 20 June 2026. Downloaded on 6/20/2026 11:52:44 PM.
This article is licensed under a Creative Commons Attribution-NonCommercial 3.0 Unported Licence.

Materials Advances Accepted Manuscript